Final Report for:

Development of Wind Speed-ups and Hurricane Hazard Maps for the United States Virgin Islands.

Prepared by:

Peter J. Vickery, Ph.D., P.E.
Fangqian Liu, Ph.D., P.E.
Francis M. Lavelle, Ph.D., P.E.
David Mizzen, P.E.

Applied Research Associates, Inc.
8537 Six Forks Rd., Suite 600
Raleigh, NC 27615

Prepared for:

STARR II
Atkins
3901 Calverton Blvd. Suite 400
Calverton, MD 20705

FEMA TASK ORDER NUMBER: 70FBR2-18-F-00000012
STARR II PROJECT NUMBER: 400000393
STARR II TRACKING NUMBER: AR S2 R02 18 T012

December 2019

1. Introduction and Background

The speed-up model being developed for the estimation of topographic speed-ups of gust wind speeds on the US Virgin Islands is based upon the model for estimating speed-ups in Hawaii developed for the Hawaii Hurricane Relief Fund (HHRF) as described in (ARA, 2001). The model was developed using empirical equations whose parameters were determined through comparisons with speed-up data obtained from wind tunnel measured on topographic models of Oahu and Kauai. The wind tunnel tests and the speed-up data from the tests are described in Chock et al. (2000) and Chock and Cochran (2005).

Figure 1and Figure 2 show the islands and the locations of the points at which speed-ups were measured in the wind tunnel. Wind speed-ups were measured for sixteen different wind directions.

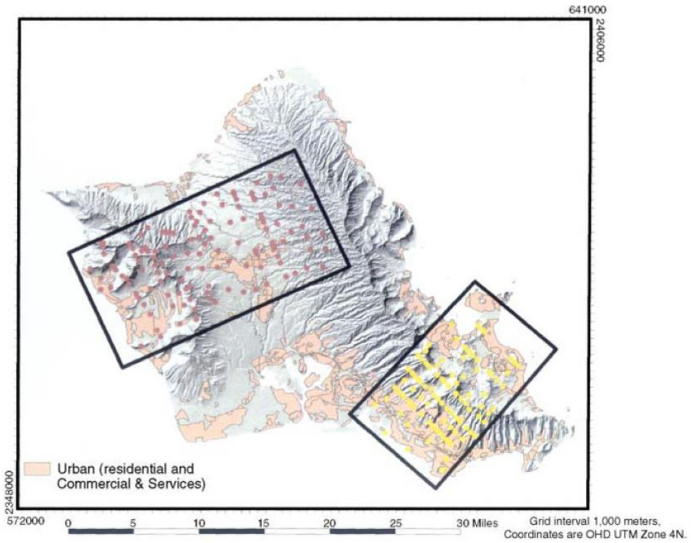

Figure 1. Map showing locations at which speed-ups were measured in the wind tunnel for the Island of Oahu.

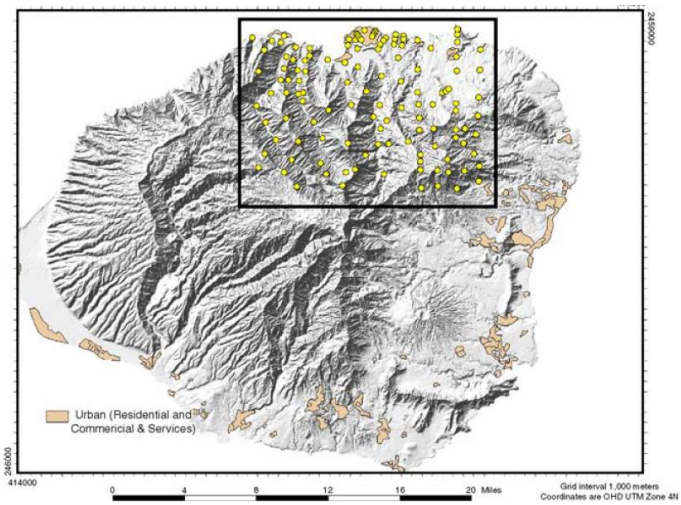

Figure 2. Map showing locations at which speed-ups were measured in the wind tunnel for the Island of Kauai.

The speed-up model developed for the HHRF was modified to improve the r^2 between the empirical model and the results of the wind tunnel tests. Through a trial and error process a significant improvement in the r^2 value of the original HHRF model was achieved.

Not all of the experimental data were used in the final comparisons as there were a number of cases where the experimental results were not deemed credible. Examples include locations ridges where the speed-ups should be a maximum for winds approaching from multiple directions, but the wind tunnel data yield speed-up factors less than unity for all directions.

The directionally directionally-dependent speed-up factor, $S(\theta)$ is computed using

$$S(\theta) = 1 + A_1 \sum_{j=1}^{16} \sum_{i=1}^{N} \left(w_r(r_i) w_\alpha(\alpha_j) \frac{dz}{dr}(r_i, \alpha_j) \right) + A_2 \sum_{j=1}^{16} \sum_{i=1}^{N} \left(w_r(r_i) w_\alpha(\alpha_j) \frac{\Delta z}{r_i}(r_i, \alpha_j) \right) \quad (1)$$

where

α is the direction measured with respect to the oncoming wind blowing from direction θ, $\Delta\alpha$ = 22.5 degrees, N is the number of radial segments, here taken as 13, and $w_\alpha(\alpha_j)$ is a directionally dependent weighting function shown in Figure 5. The constant A_1 is equal to 2.0. The constant A_2 is equal to 0.75 when the numerator in the second term of Equation 1 is negative and 0 otherwise. $w_r(r_i)$ is a weighting function that decreases with increasing distance from the point at which the speed-up is being computed, and is defined as

$$w_r(r_i) = \frac{\frac{1}{\left(1 + a_1 \left(\frac{r_i}{z_E}\right)^{a_2}\right)}}{\sum_{i=1}^{N} \left(\frac{1}{1 + a_1 \left(\frac{r_i}{z_E}\right)^{a_2}} \right)} \quad (2)$$

The constants a_1 and a_2 are 0.8 and 1.5, respectively, and z_E is the elevation above sea level at the location of the point for which the speed-ups are being computed. The minimum value of z_E is set to 1.0 m. The radius, r_i, is equal to $i\Delta r$, where Δr is 200m. The local slope, $\frac{dz}{dr}(r_i, \alpha_j)$ is calculated in the direction of the radial using

$$\frac{dz}{dr}(r_i, \alpha_j) = \frac{\delta z}{\delta r} = \frac{z_i - z_{i+1}}{r_i - r_{i+1}} \quad (3)$$

The global slope, $\frac{\Delta z}{r_i}(r_i, \alpha_j)$ is calculated in the direction of the radial using

$$\frac{\Delta z}{r_i}(r_i, \alpha_j) = \frac{z_E - z_i}{r_i} \quad (4)$$

As implemented in Equation 1, both the local and global the slopes are positive downwards.

The form of the weighting function, $w_\alpha(\alpha_j)$, is such that the speed-up increases with increasing slope in front of the point of interest. If the slope to the immediate left or right of the site (90 degrees or 270 degrees) is positive (i.e., downhill) the speed-up is decreased as the wind is able to go around the location. Conversely, if the slope is negative (e.g., the walls of a valley) the wind speed is increased due to the

effects of channeling. The sign of the function for α_j=180 degrees (i.e., radial directly upwind) is positive, decreasing the speed-up as the slope is negative (uphill), but has a lesser magnitude than for the direction where winds are approaching the point. For very steep negative slopes the speed-up becomes less than 1, since the flow separates and locations on the hill are in a wake region of recirculation. The same applies on the leeward side of steep hills For points located at or near a ridge, or hill top, the positive slope behind the point increases the speed-up such that, all else being equal, a ridge produces a maximum speed-up.

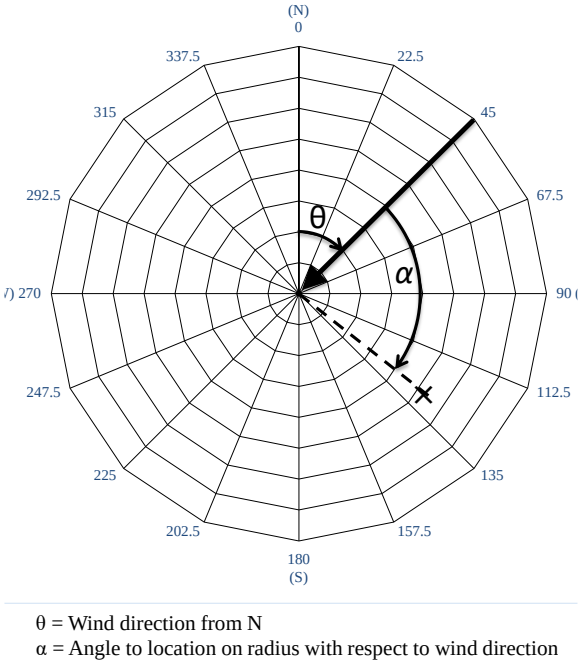

Figure 3. Definition of angles for wind speed-up calculations.

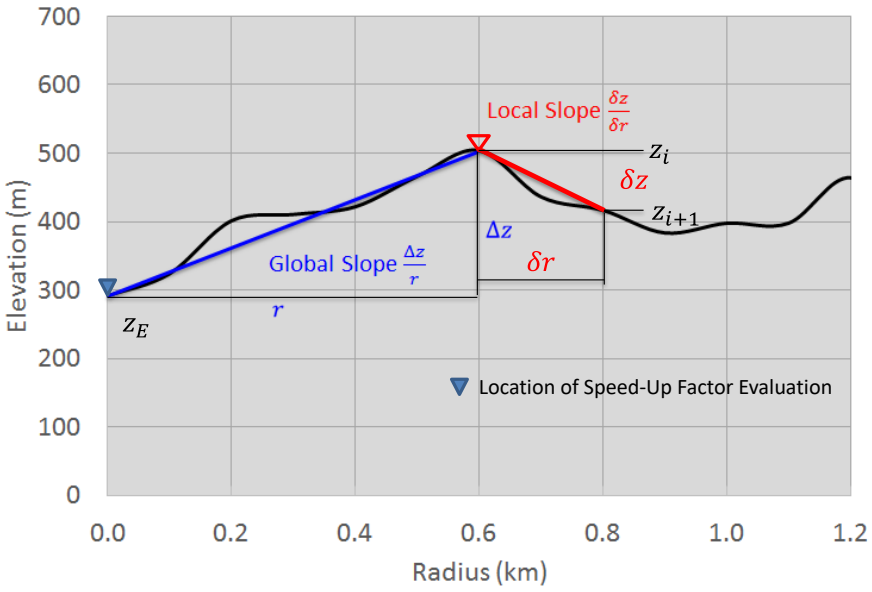

Figure 4. Definition of slopes.

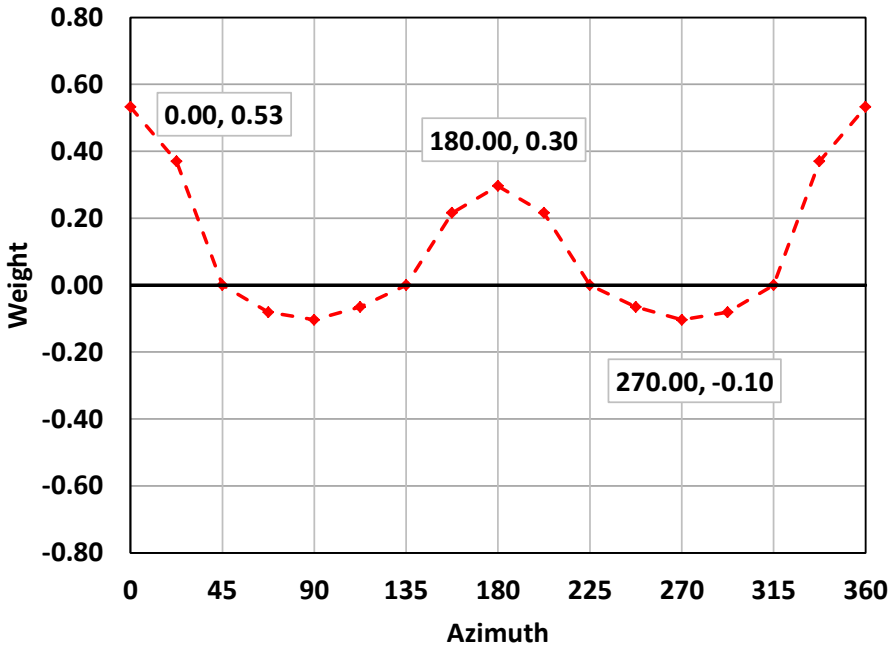

Figure 5. Directional weighting function $w_\alpha(\alpha_j)$.

Using equations (1) through (3), wind speed-ups were produced for sixteen directions at increments of 22.5 degrees. Figure 6 presents a comparison of speed-ups produced by the Chock and Cochran (2005) model and the model presented herein for a single point on Oahu. The model presented herein performs better than the Chock and Cochran (2005) model for winds approaching from about 200 degrees to about 290 degrees. Both models understate the reduction in wind speed for easterly through southerly directions and both models underestimate the peak speed-ups. As pointed out by Chock and Cochran (2005) their predictive model is less sensitive to severe changes in wind speed over a single 22.5° directional interval. The same is true for the model developed here.

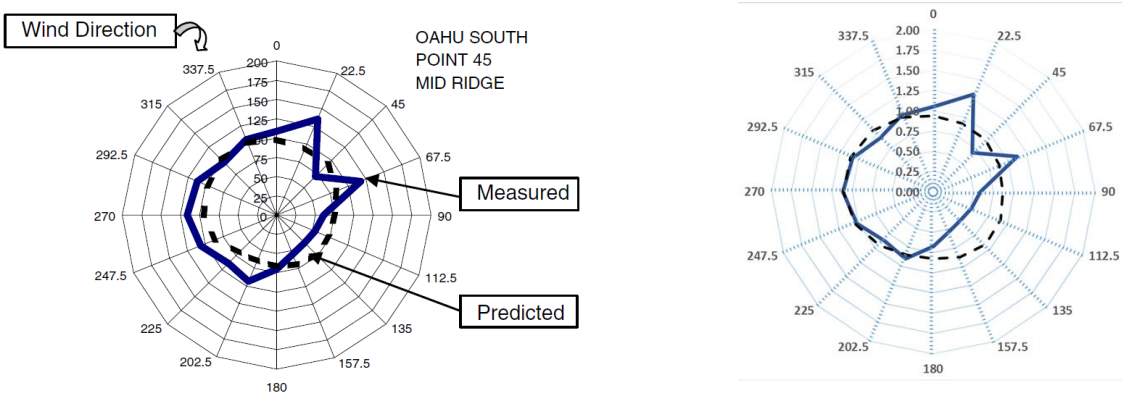

Figure 6. Comparisons of modeled and measured speed-ups on a mid-ridge location on Oahu from Chock and Cochran (left) and the current model (right)

Figure 7 presents the results of regression plots comparing the speed-up factors generated by the model and those obtained from the wind tunnel tests. The regression plots are given for two cases, one where the model results are presented without modification and the other where the model results are capped at a

maximum of 2.0 and a minimum of 0.4. The model with the limits produces a slightly higher r^2 than the unlimited model. The regression plots include data for all wind directions, not just the maximum speed-up.

Figure 8 and Figure 9 show the data presented in Figure 7 in the form of 2-D and 3-D histograms. The histograms show most of the model-experimental data pairs fall very near the diagonal.

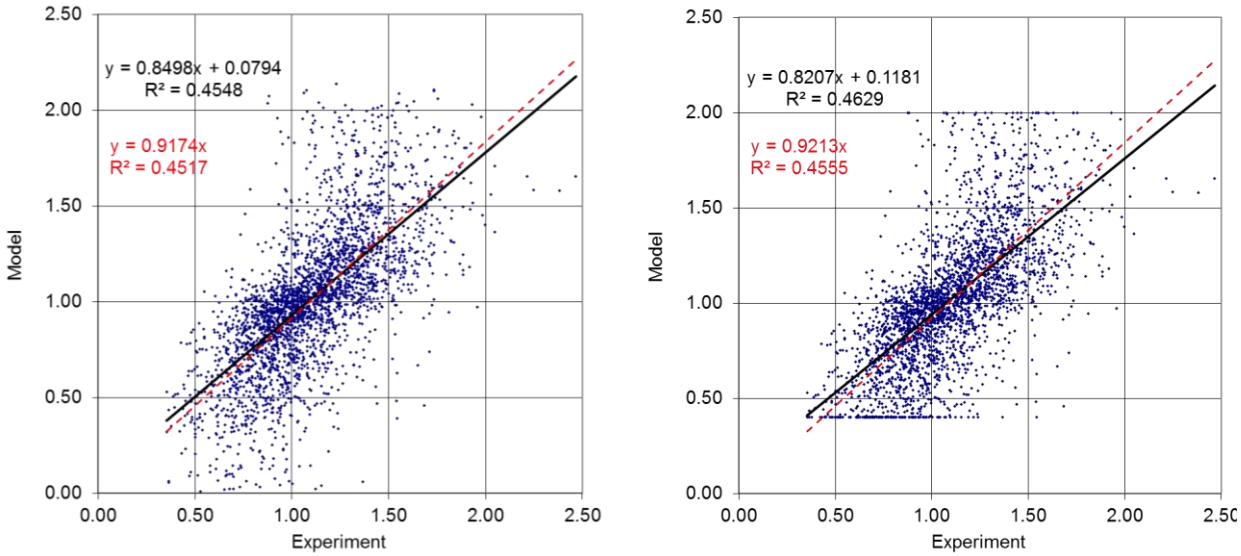

Figure 7. Comparison of model generated and measured topographic speed-ups. Left plot shows model results without caps, right plot shows results with caps

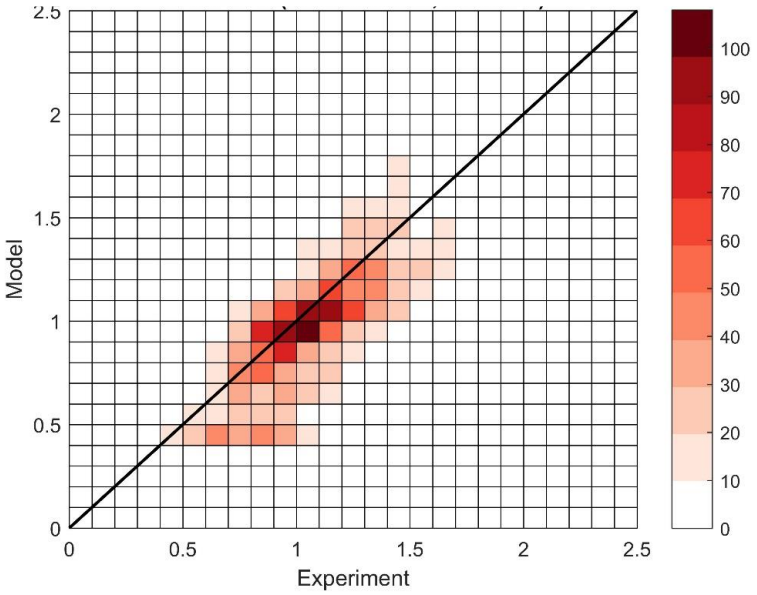

Figure 8. 2-D histogram showing the relative frequency of modeled-measured pairs of speed-up data presented in bins of 0.1. Note the darkest colors (highest frequency) appear near the diagonal.

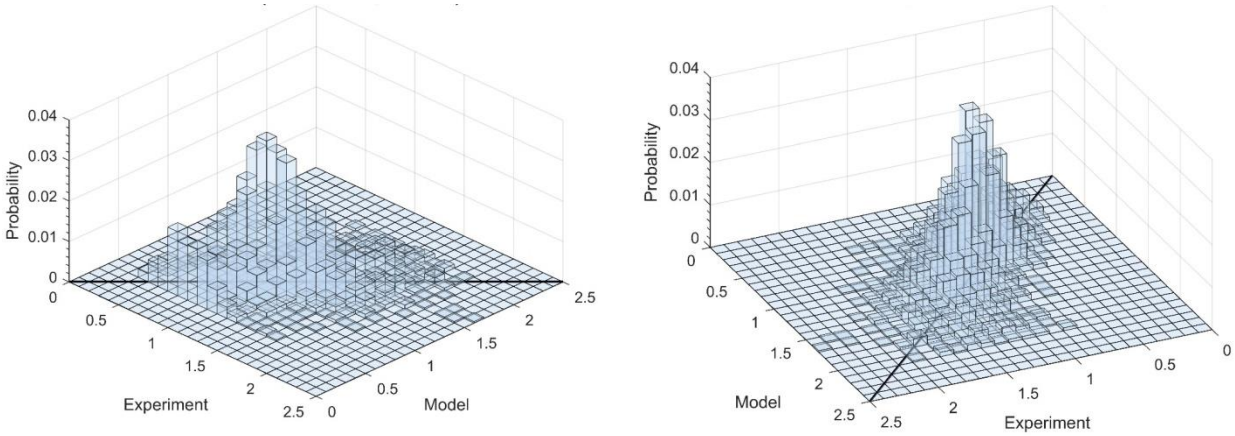

Figure 9. 3-D histograms showing the relative frequency of modeled-measured pairs of speed-up data presented in bins of 0.1. Note the darkest colors (highest frequency) appear near the diagonal.

Chock and Cochran (2005) and Chock et al. (2005) also developed a model for topographic speed-ups using the wind tunnel speed-up data. The results from their model are incorporated into the design wind speed maps for the Hawaiian Islands as given in ASCE 7-16. Figure 10 presents a comparison of modeled and observed speed-ups from Chock et al. (2005) and/or Chock and Cochran (2006).

The comparison is presented incorrectly with the experimental (measured) results on the vertical axis; consequently the true r^2 of the model is unknown. If a regression line is forced through the origin, the r^2 will not be the same if the axes are switched. The r^2 will only be the same if the regression line is not constrained. Furthermore, as stated in Chock et al. (2005), experimental values from ridges were removed when their model was developed.

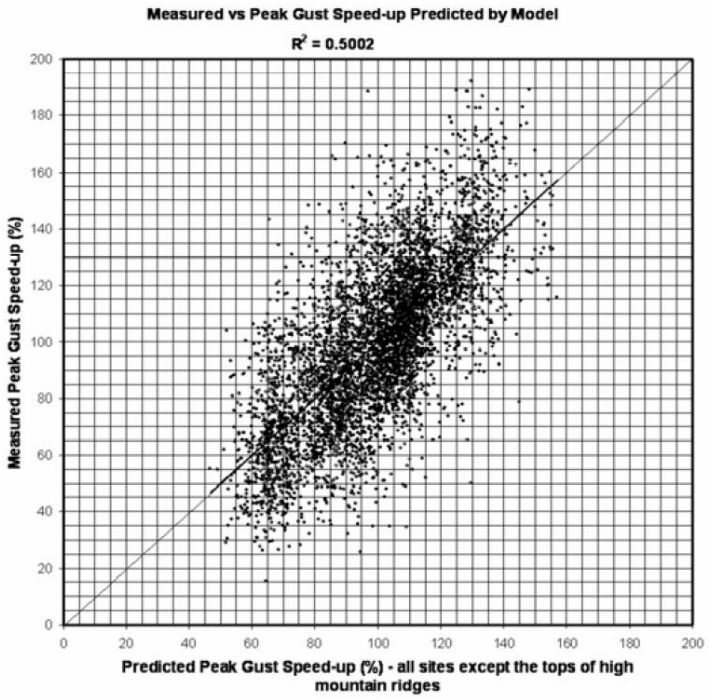

***Figure 10. Comparison of model generated and measured topographic speed-ups.* (*Chock et al., 2005*).**

Chock and Cochran (2006) suggest that using the ASCE 7 provisions for simple hills, ridges and escarpments would obtain a maximum r^2 in the range of 0.20 to 0.30 when applied to the complex topography of Hawaii. The same would likely apply to the complex topography of the USVI.

Figure 11 presents the maximum wind speed-ups over all directions for the Island of Oahu presented in Chock et al. (2005). On the far western peninsula the contours of speed-up run perpendicular to the ridge rather than parallel to the ridge. Similarly, the contours of the speed-ups do not reflect the maxima that would be expected along the ridge running approximately north-south on the east side of the Island.

The maximum values of the speed-ups produced by the model developed herein are presented in Figure 12. The highest values of the speed-up factors follow ridges lines, a result that is qualitatively consistent with the speed-up models for isolated, simple hills, 2-D ridges, etc. in ASCE 7, which yield maximum speed-ups for ridges.

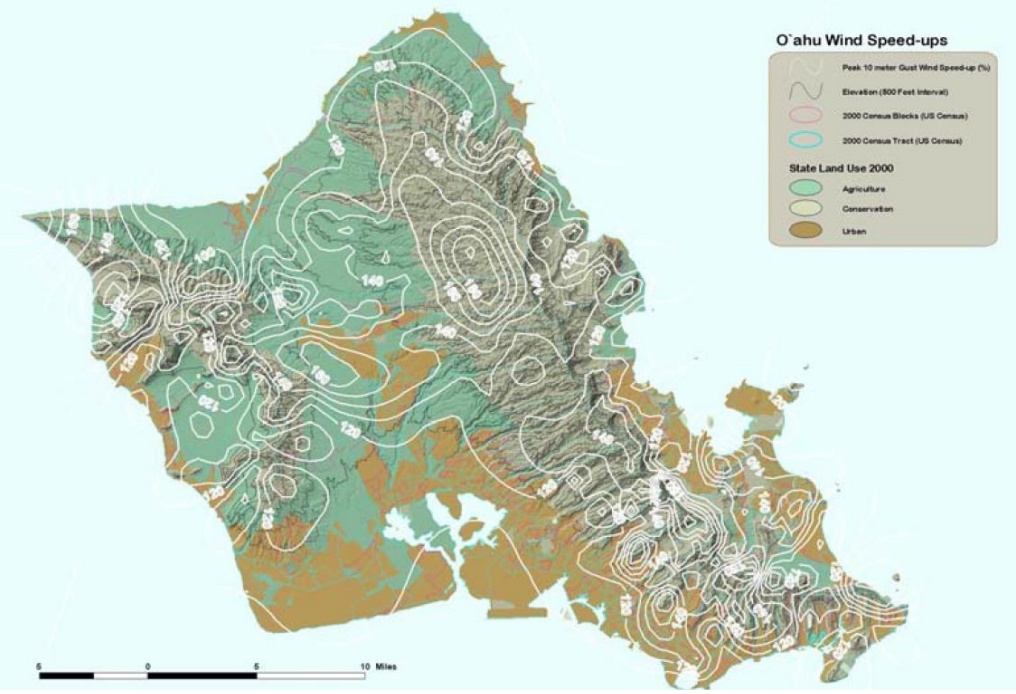

Figure 11. Map of maximum (from all directions) speed-up factors from Chock et al. (2005).

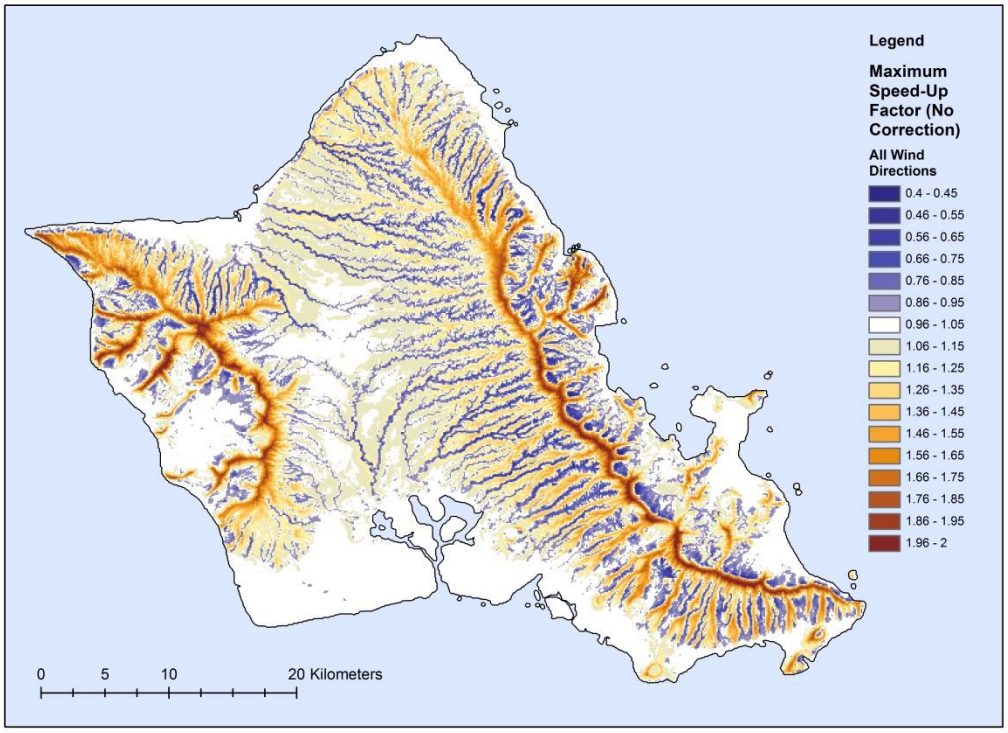

Figure 12. Map of maximum speed-up factors produced by current model.

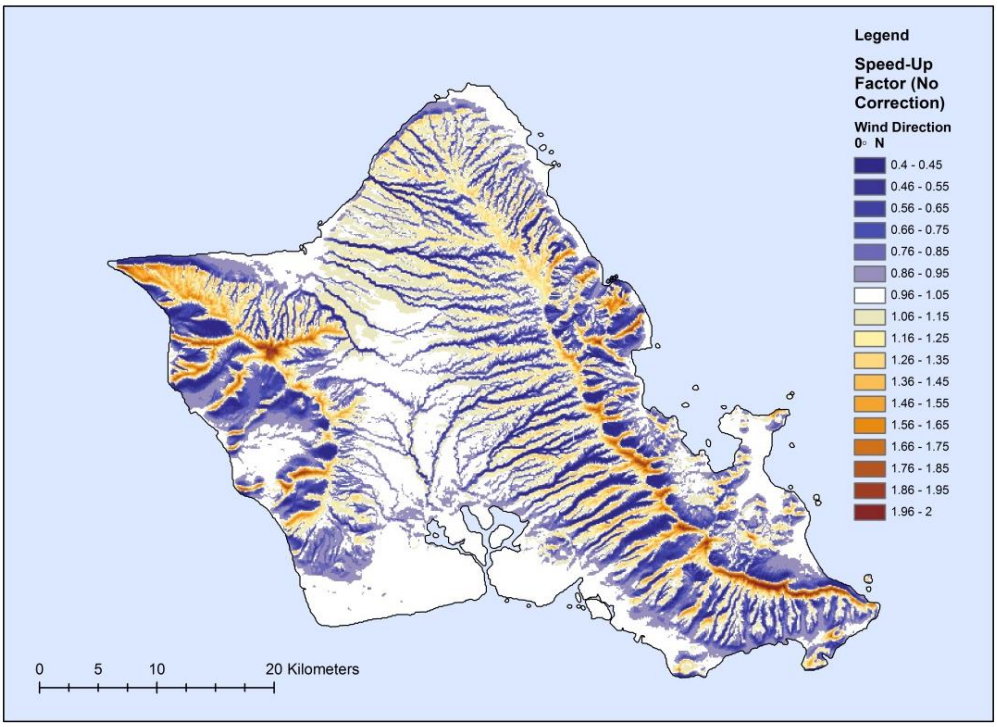

Figure 13. Speed-up factors for winds approaching from the north (from top of page)

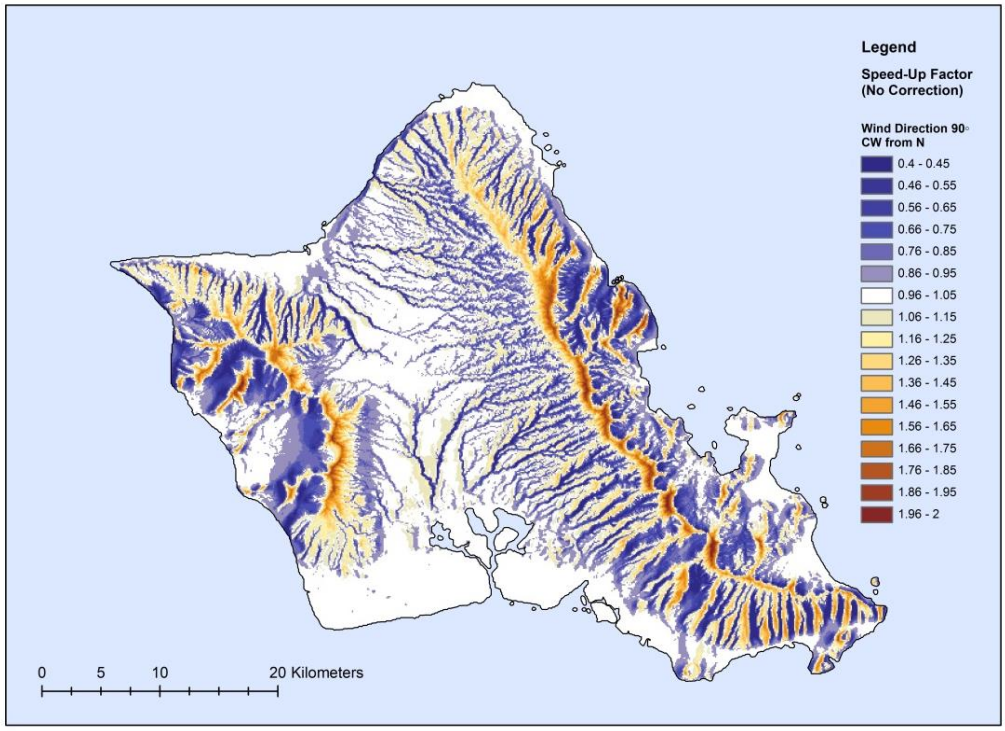

Figure 14. Speed-up factors for winds approaching from the east (from right side of page)

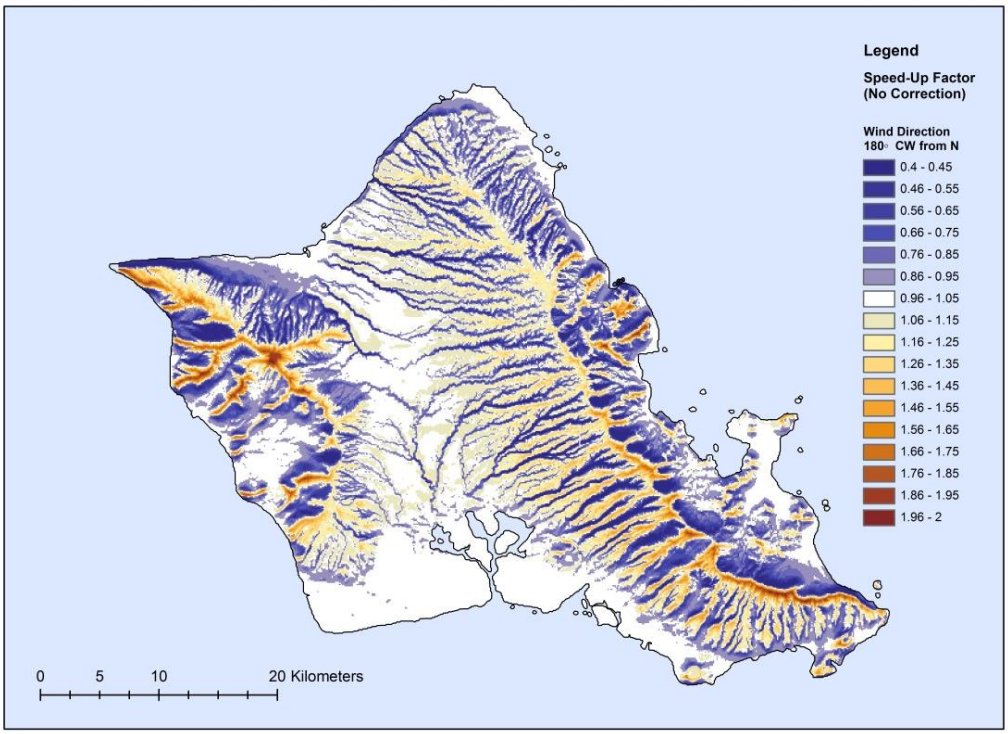

Figure 15. Speed-up factors for winds approaching from the south (from bottom of page).

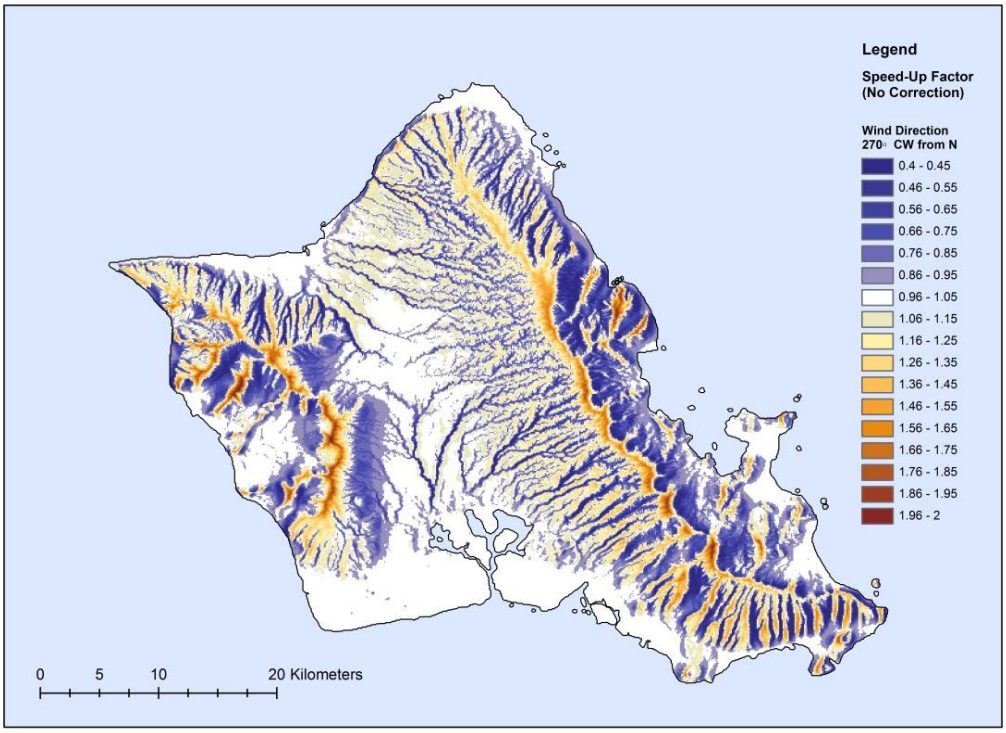

Figure 16. Speed-up factors for winds approaching from the west (from left side of page).

2. USVI Topographic Speed-ups

Topographic speed-ups on the United States Virgin Islands (USVI)were computed using the empirical models developed for Hawaii as discussed in Section 1. The digital elevation model (DEM) used for developing the topographic speed-up factors for the USVI was obtained from the USGS web site (https://viewer.nationalmap.gov/basic/?basemap=b1&category=ned,nedsrc&title=3DEP%20View). The original horizontal resolution of the DEM is 1/3 arc second (~ 10 m). Wind speed-ups are computed at every point on a 100 m grid rather than at each 10 m DEM point (i.e., the DEM used to compute the wind-speeds used a final grid with a 100 m resolution). A total of 36,982 wind speed-up points were used to model the USVI. 7,586 grid points are on the Island of St. Thomas, 5,529 on the Island of St. John and 21,921 points are on St. Croix. The remainder of the points are distributed over the smaller islands. As in the case of the Hawaii speed-ups, were computed for sixteen different wind directions at increments of 22.5°.

The DEM's for the USVI are shown in Figure 17. The maximum speed-ups over all sixteen directions are presented in Figure 18. A large area of little or no speed-up is evident on the south side of St. Croix where the topography is very flat.

Topographic speed-up factors on a direction-by-direction basis are presented in Appendix A. Example single wind direction cases are presented in Figure 19 and Figure 20 for winds approaching from the north and south respectively. As in the case of Hawaii, areas with steep slopes, either on the windward or leeward side of ridges experience speed-ups less than one due to the wind separating over the ridge and

creating regions of recirculation (see for example, Berg et al., 2011 and Bechmann et al., 2011). The areas of reduced wind speed are particularly evident on the Islands of St. John and St. Thomas. The highest speed-ups occur near ridges and slopes where the flow does not separate. Valleys are also regions of reduced speeds when the wind is not approaching from the direction of the valley.

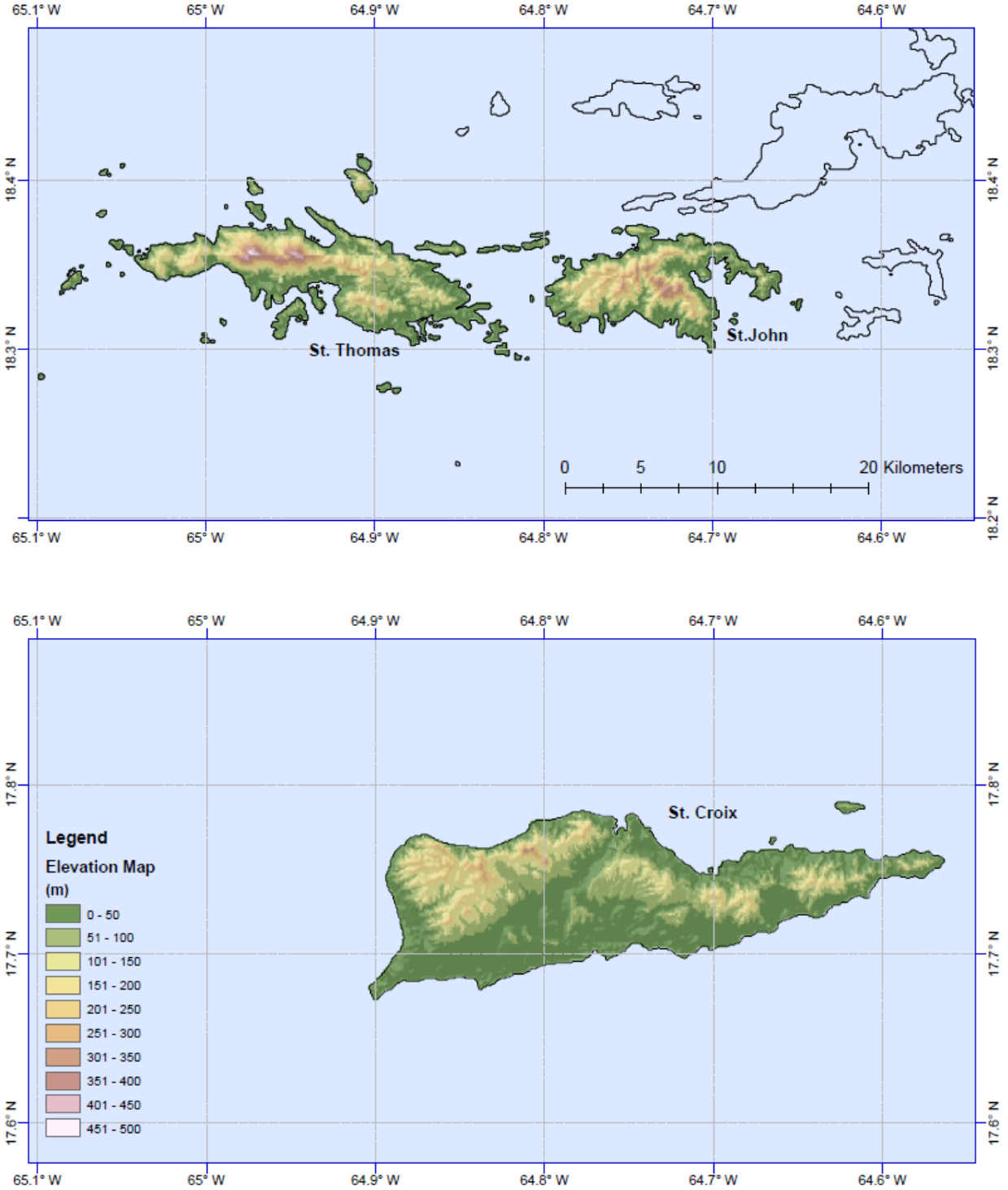

Figure 17. Elevation maps of the USVI developed from DEM used for topographic speed-up modeling.

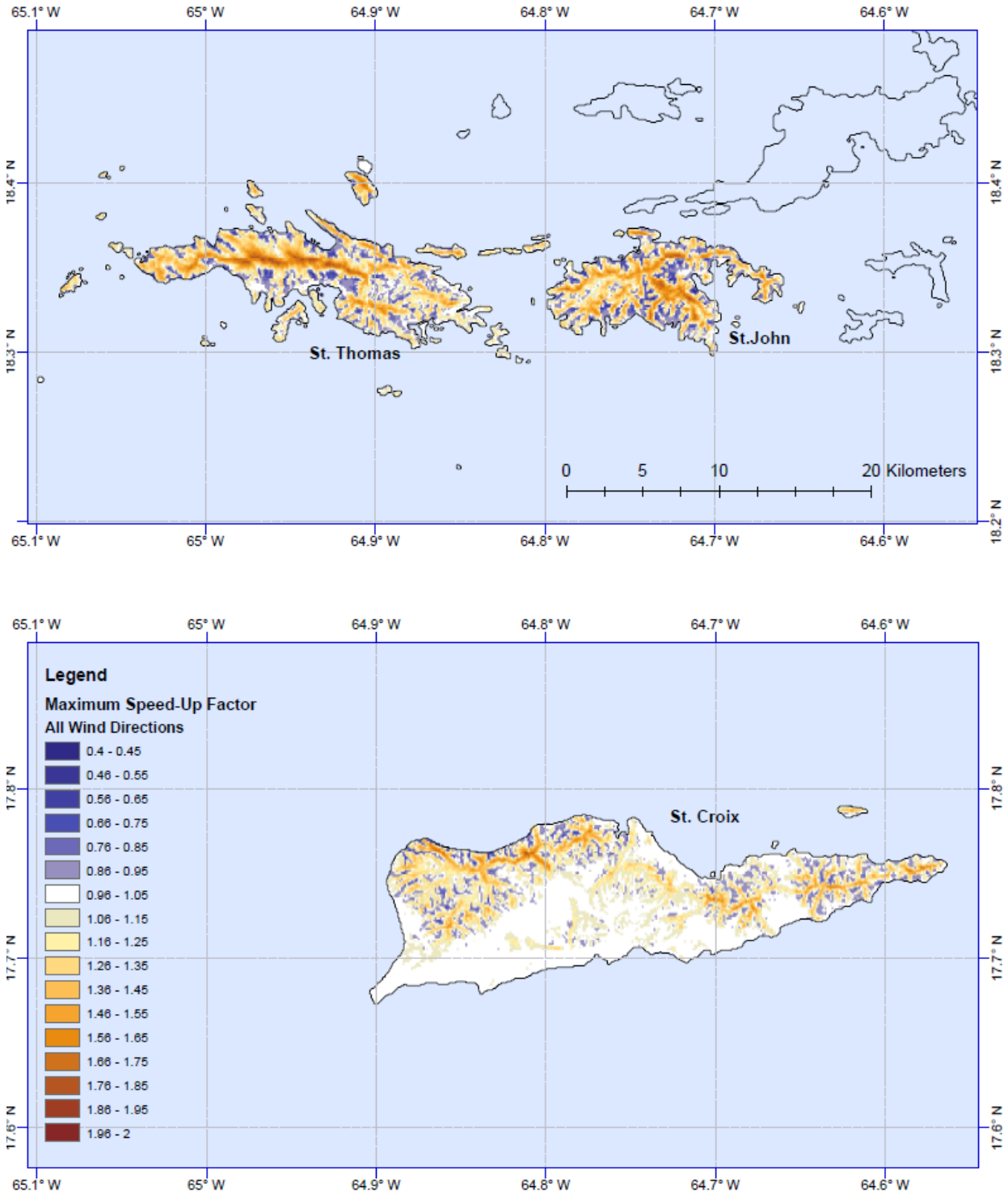

Figure 18. Maximum topographic speed-up factors for the USVI.

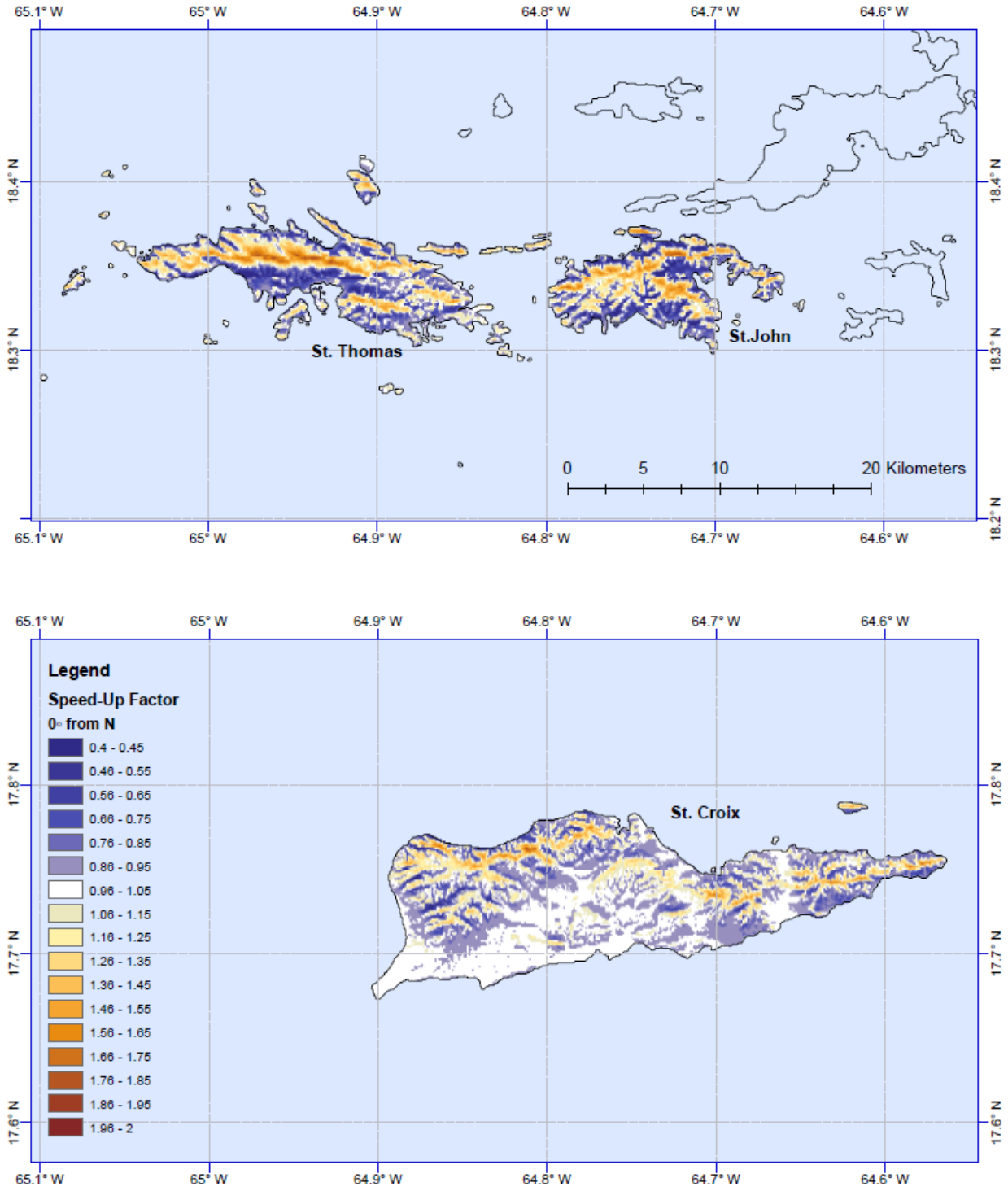

Figure 19. Wind speed-ups for winds approaching from the north (0°)

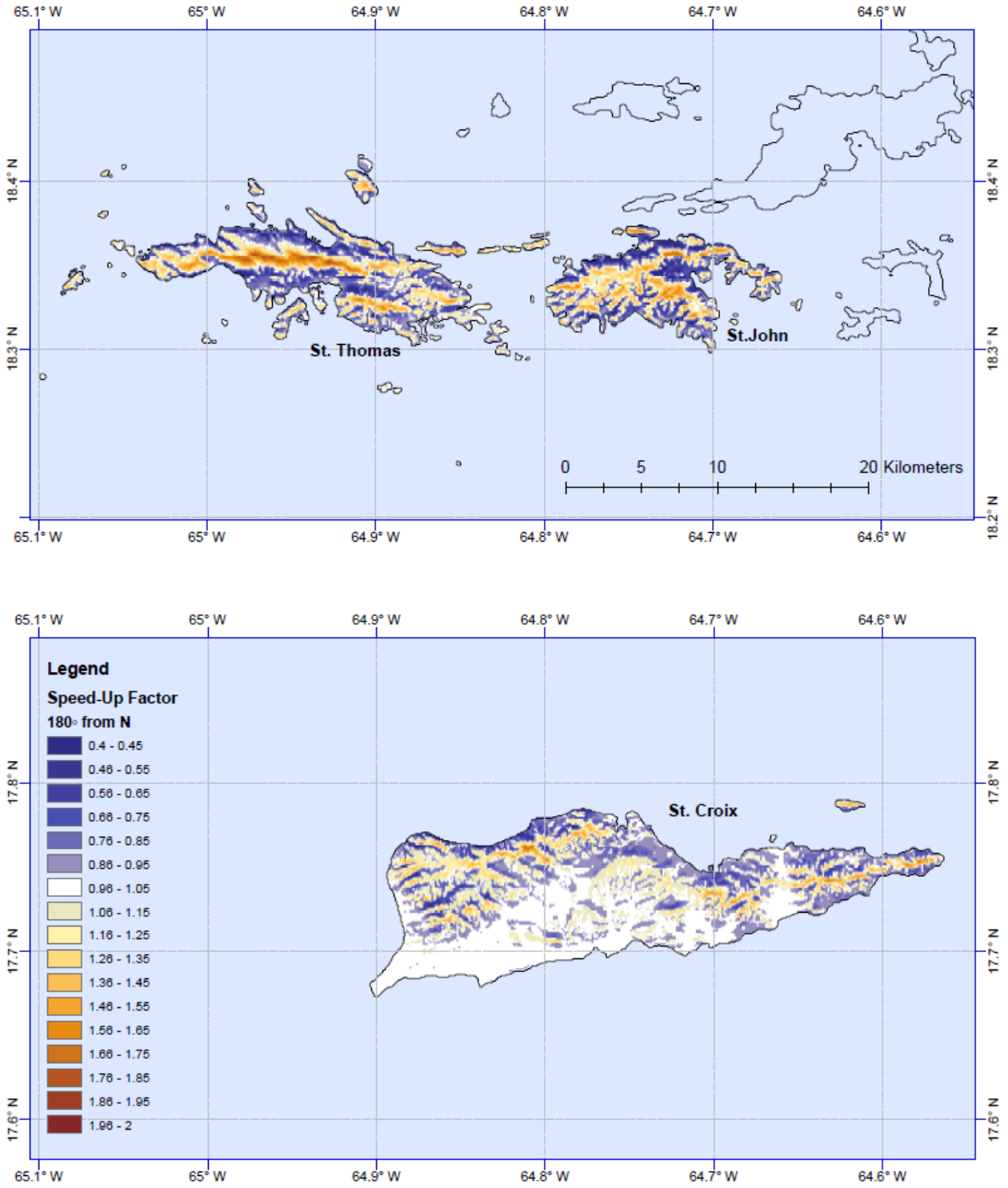

Figure 20. Wind speed-ups for winds approaching from the south (180°)

3. Hurricane Modeling and Development of Wind Maps

The hurricane simulation for the USVI uses the hurricane simulation model described in Vickery and Wadhera (2008). This is the same model that was used to develop the design wind speeds for the USVI given in ASCE 7-10 and ASCE 7-16. The wind grid used to for the computation of hurricane winds is shown in Figure 21. There are a total of 14,236 wind grid points distributed over the main and surrounding islands. Near the coast the grid spacing is about 90 m, and then increases to a spacing of about 360 m away from the coast.

The hurricane simulation produces time histories of wind speed and directions at each wind grid point using a 100,000 year simulation of synthetic hurricanes. The 100,000 years of simulated tracks are the same tracks used to develop the wind speeds given in ASCE 7-16. Wind speeds and directions are computed every 10-minutes. Each wind grid point is mapped to the closest location for which speed-ups were computed. In many cases the wind grid points align with a wind speed-up point. Using the time series of wind speeds and directions from the hurricane simulations, the wind speed associated with a given direction is mapped to a 22.5° sector, and the simulated gust wind speed is multiplied by the speed-up factor associated with the appropriate direction. The maximum wind speed, including the effect of the topographic speed-ups is retained and used in the extreme value analysis to develop a wind hazard curve for each point. The wind speed used to develop the maps uses the results of the wind hazard curves computed with the effect of topography included unless the wind hazard curve developed for flat open terrain is greater. This is consistent with the provisions of ASCE 7 that state the effects of shielding shall not be considered. All wind speeds are valid for open terrain conditions.

Upon completion of the 100,000-year simulation, the wind speed data are rank ordered and then used to define the wind speed probability distribution, $P(v>V)$, conditional on a storm having passed within 250 km a grid point and producing a peak gust wind speed at ground level in flat open terrain at the grid point of at least 20 mph. The probability that the tropical cyclone wind speed (independent of direction) is exceeded during time period t is

$$P_t(v > V) = 1 - \sum_{x=0}^{\infty} P(v < V \mid x)\, p_t(x) \tag{5}$$

where $P(v < V \mid x)$ is the probability that velocity v is less than V given that x storms occur, and $p_t(x)$ is the probability of x storms occurring during time period t. $P(v < V \mid x)$ is obtained by interpolating from the rank ordered wind speed data. From Equation (5), with $p_t(x)$ defined as Poisson and defining t as one year, the annual probability of exceeding a given wind speed is:

$$P_a(v > V) = 1 - \exp[-\lambda P(v > V)] \tag{6}$$

where λ represents the average annual number of storms approaching within 250 km of the site and producing a minimum 20 mph peak gust wind speed (i.e., the annual occurrence rate).

The model results include the effect of uncertainties in wind speed. The wind speed uncertainty term is the same as that used in the development of the ASCE 7-10 and ASCE 7-16 wind speed maps. This error term increases the 100-year return period wind speed by a few percent. The effect of the error term on the percentage increase of the nominal wind speed increases with increasing return period. The wind speed

uncertainty term is modeled using a multiplicative term with a mean of 1.0 and a standard deviation, σ, of 0.10.

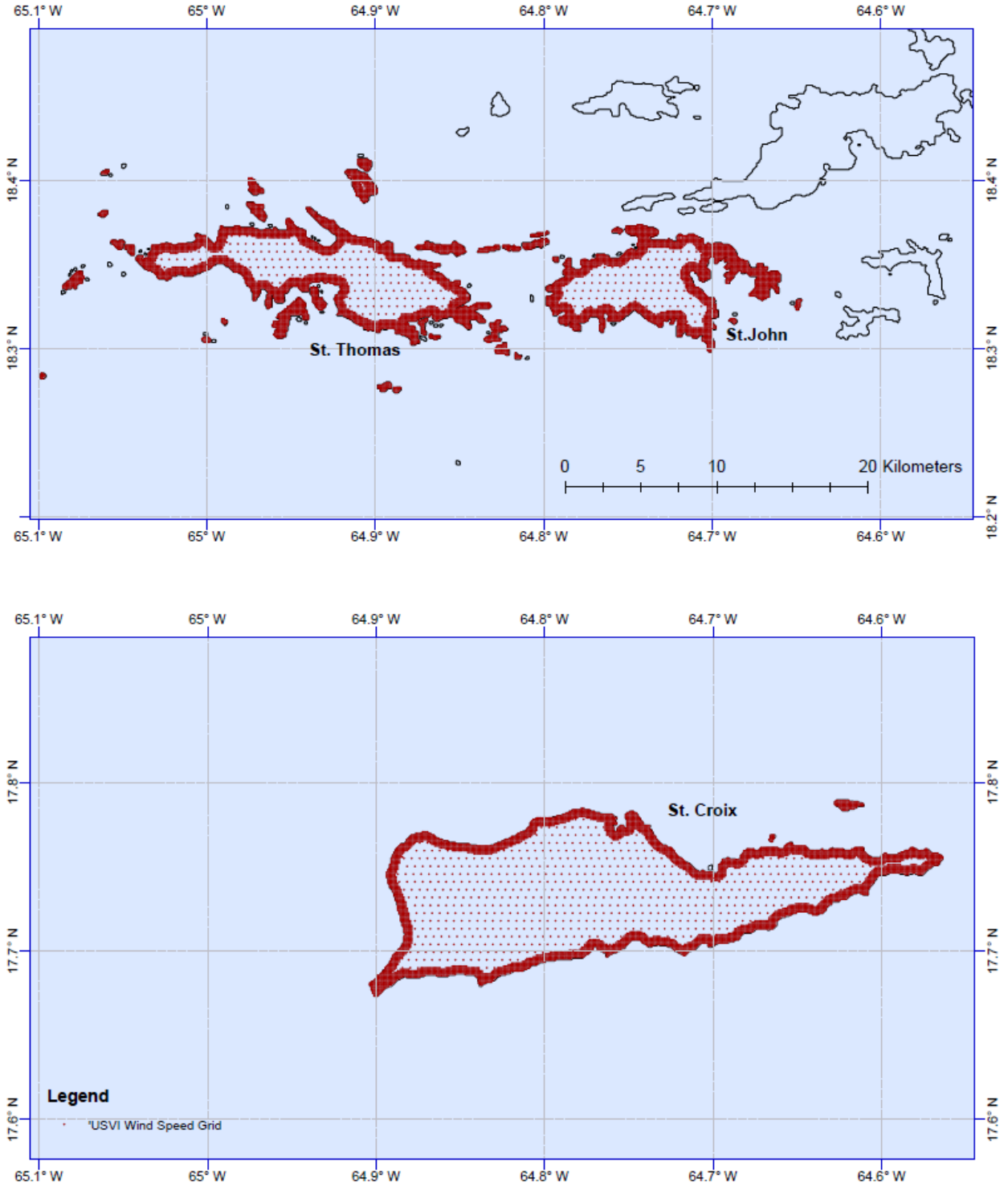

Figure 21. Grid points on the USVI used for the computation of hurricane induced wind speeds and directions.

Figure 22 through Figure 26 present maps of 100-, 300-, 700-, 1,700- and 3,000-year return period wind speeds for the USVI. As seen in the figures, the range of wind speeds on the islands when topography is included is significant. For example, for the 700-year case the wind speeds range from 162 mph to 291 mph, whereas the single value for the USVI specified in ASCE 7-16 is 165 mph.

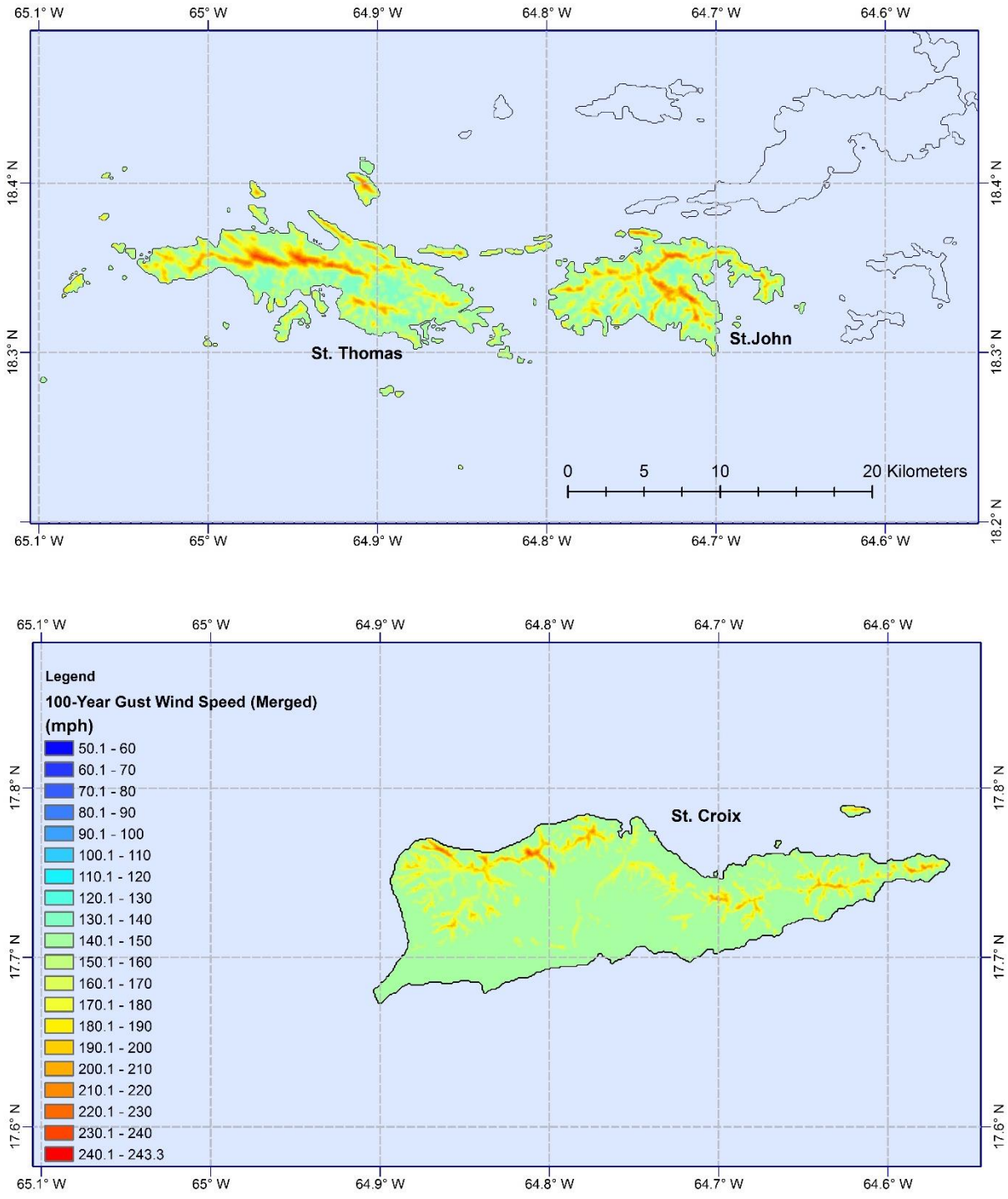

Figure 22. 100-year return period 3-second gust wind speeds for the USVI including the effects of topographic speed-ups. Wind speeds are valid for a height of 10 m in open terrain.

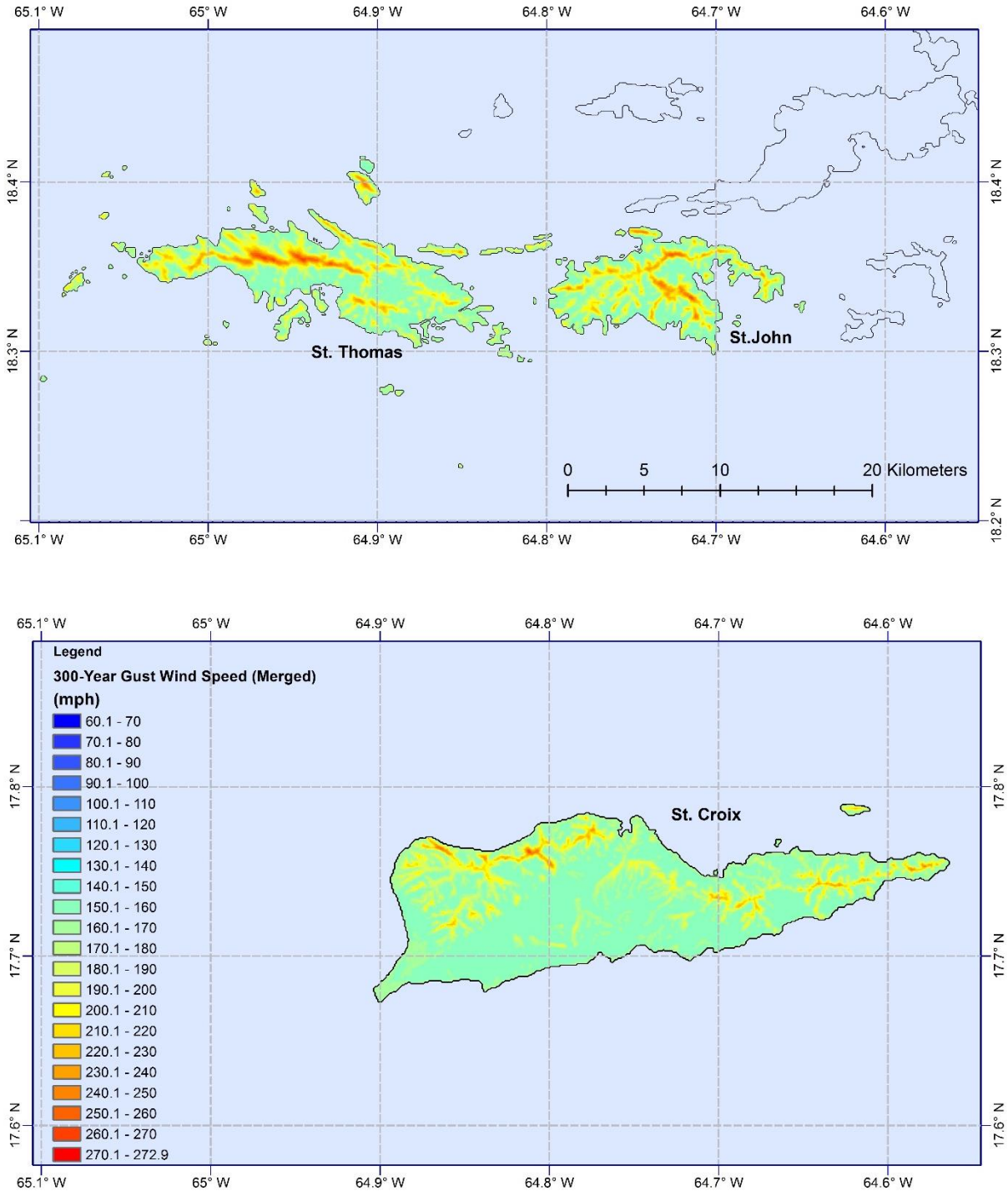

Figure 23. 300-year return period 3-second gust wind speeds for the USVI including the effects of topographic speed-ups. Wind speeds are valid for a height of 10 m in open terrain.

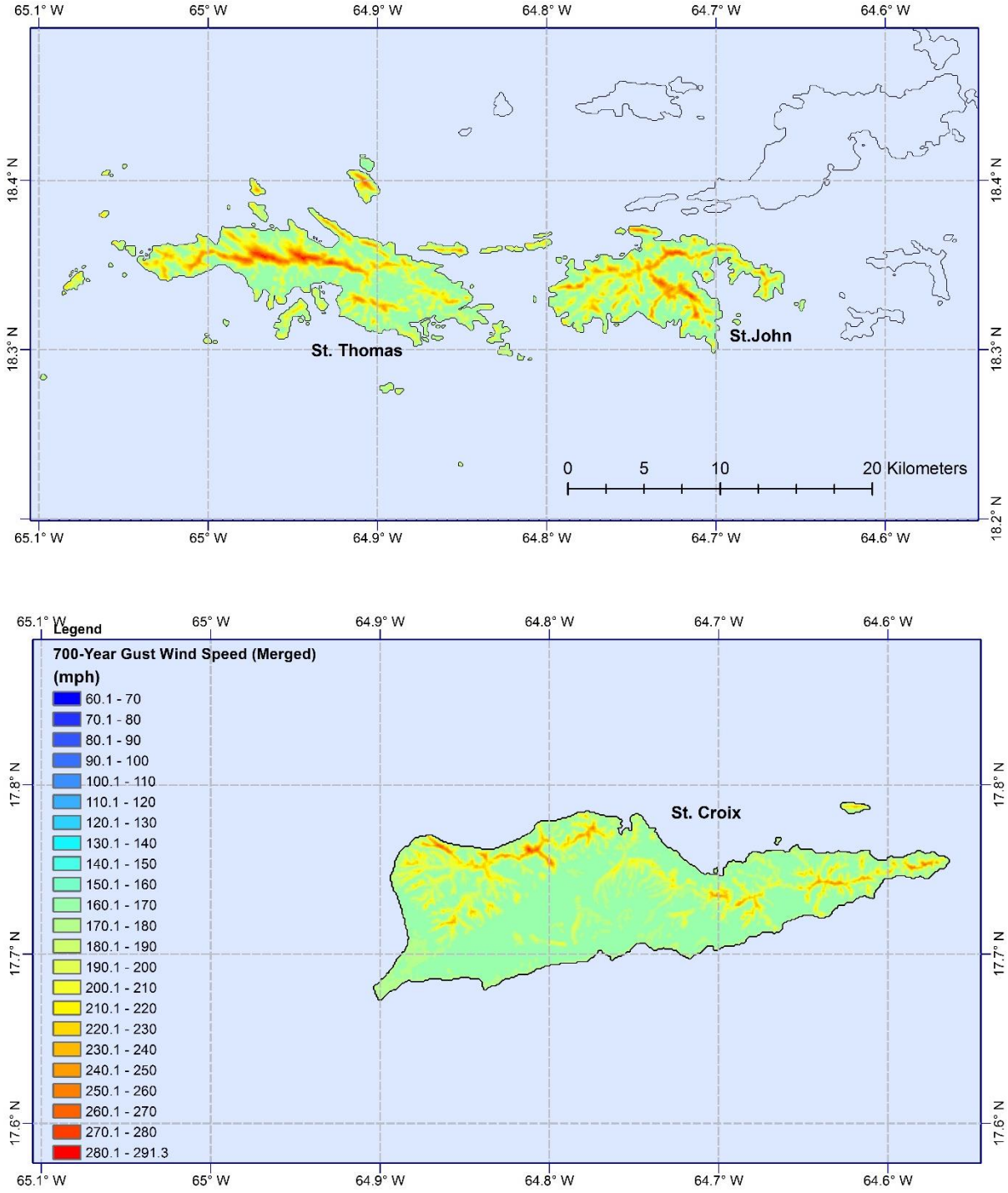

Figure 24. 700-year return period 3-second gust wind speeds for the USVI including the effects of topographic speed-ups. Wind speeds are valid for a height of 10 m in open terrain.

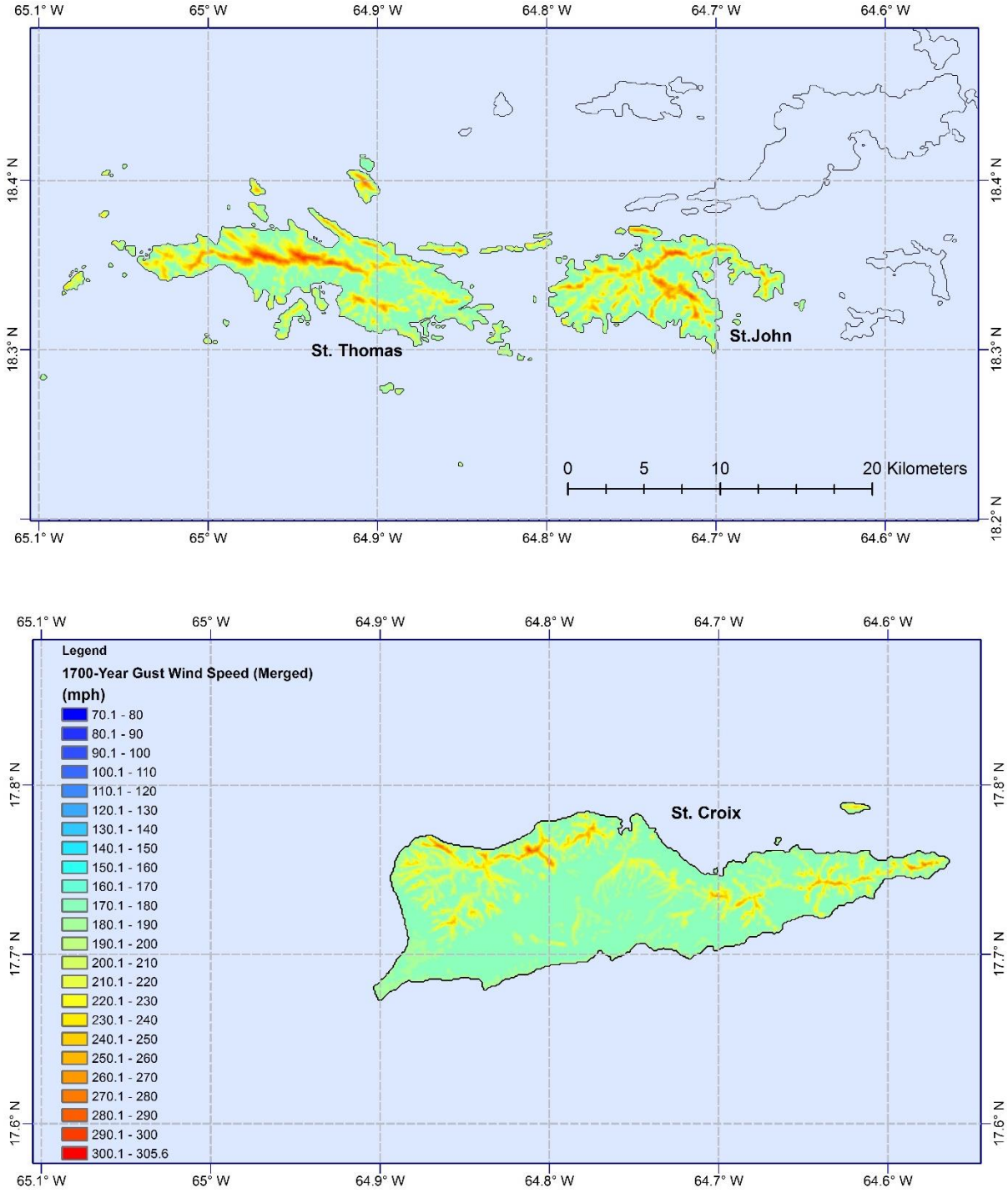

Figure 25. 1,700-year return period 3-second gust wind speeds for the USVI including the effects of topographic speed-ups. Wind speeds are valid for a height of 10 m in open terrain.

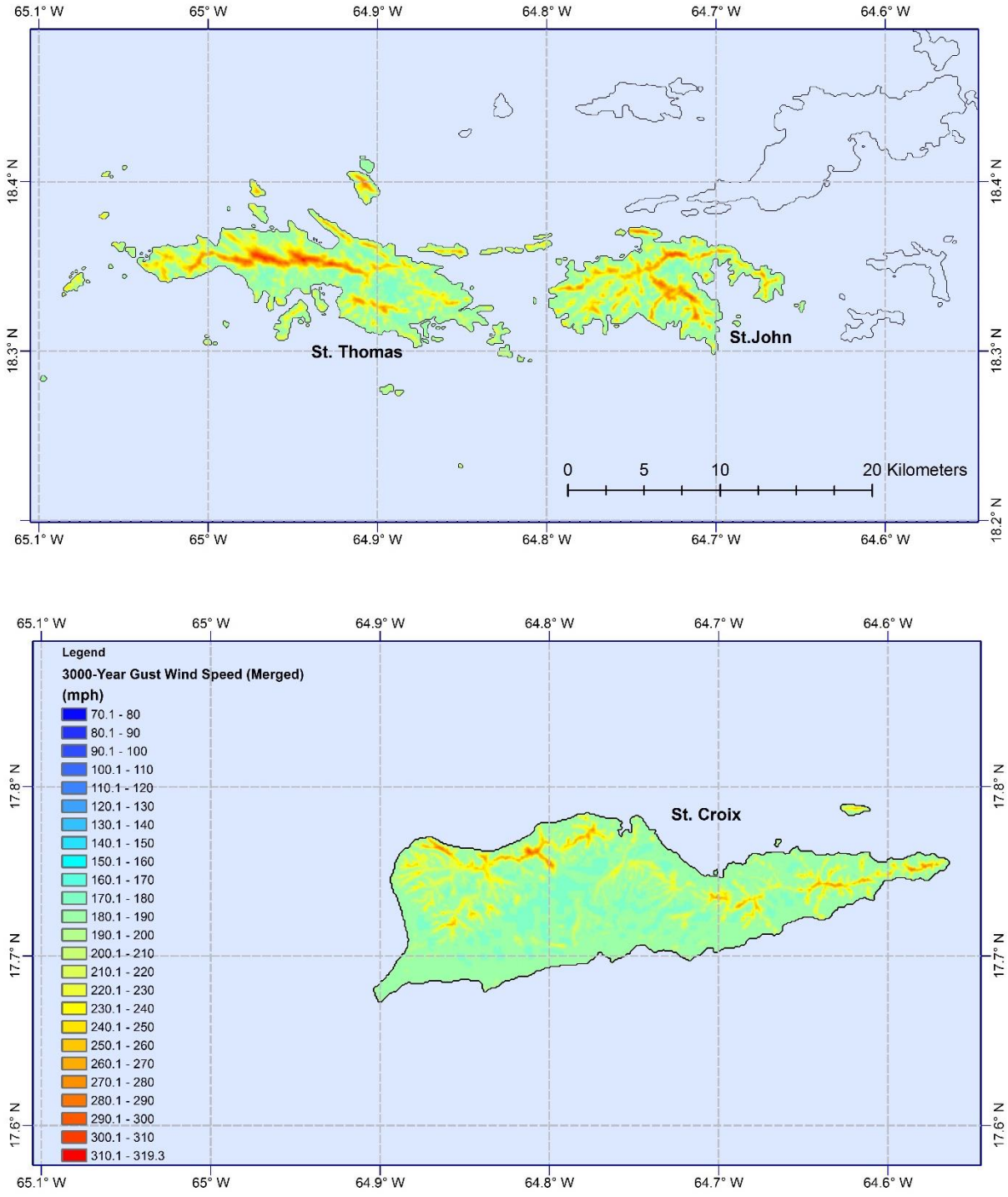

Figure 26. 3,000-year return period 3-second gust wind speeds for the USVI including the effects of topographic speed-ups. Wind speeds are valid for a height of 10 m in open terrain.

4. Wind Speeds Produced by Hurricanes Irma and Maria (2017)

Estimates of wind speeds produced by Hurricanes Irma and Maria on the USVI, including the effects of topography, were developed using the hurricane tracks developed for FEMA and NIST in 2017. These data were combined with the topographic speed-up models developed herein. Maps of the wind speeds were developed for both flat open terrain conditions and with the effect of topography. In the case where topographic speed-ups are included, the wind speeds are not constrained to be equal to or greater than those associated with flat open terrain. Consequently, when topography is considered, some locations have maximum wind speeds that are less than those which would have been estimated assuming flat open terrain over the entire island.

Figure 27 shows the track of Hurricane Irma with respect to the USVI. As can be seen in Figure 27 the track passes to the northeast of the Islands, closest to St. John. Also shown in Figure 27 are the maximum wind speeds (including the effect of topographic speed-up) on all the Islands comprising the USVI. Wind speeds are given in the form of peak (3-second) gust values at a height of 10 m in open terrain conditions. Figure 28 presents a close-up view of the peak gust wind speeds at a height of 10 m in flat open terrain Figure 29 presents a close-up view of the peak gust wind speeds at a height of 10 m in open terrain including the effects of topography. A comparison of the two sets of maps shows the very significant effect topography has on both reducing and increasing the gust wind speeds compared to the open terrain cases. The maximum and minimum wind speeds with and without the effects of topography are summarized in Table 1.

Table 1. Modeled maximum and minimum gust wind speeds on the three main islands of the USVI caused by Hurricane Irma, showing the effect of topography.

Island	Flat Open Terrain		Open Terrain with Topography	
	Minimum (mph)	Maximum (mph)	Minimum (mph)	Maximum (mph)
St. John	145.7	174.1	59.0	266.0
St. Thomas	127.0	156.8	53.0	231.2
St. Croix	56.3	75.3	24.7	112.0

Figure 30 shows the track of Hurricane Maria with respect to the USVI. As can be seen in Figure 30 the track passes to the southwest of the Islands, closest to St. Croix. Also shown in Figure 30 are the maximum wind speeds (including the effect of topographic speed-up) on all the Islands comprising the USVI. Wind speeds are given in the form of peak (3-second) gust values at a height of 10 m in open terrain conditions. Figure 31 presents a close-up view of the peak gust wind speeds at a height of 10 m in flat open terrain Figure 32 presents a close-up view of the peak gust wind speeds at a height of 10 m in open terrain including the effects of topography. A comparison of the two sets of maps shows the very significant effect topography has on both reducing and increasing the gust wind speeds compared to the open terrain cases. The maximum and minimum wind speeds with and without the effects of topography are summarized in Table 2.

Table 2. Modeled maximum and minimum gust wind speeds on the three main islands of the USVI caused by Hurricane Maria, showing the effect of topography.

Island	Flat Open Terrain		Open Terrain with Topography	
	Minimum (mph)	Maximum (mph)	Minimum (mph)	Maximum (mph)
St. John	83.4	93.9	33.6	145.3
St. Thomas	90.2	102.7	36.3	150.3
St. Croix	105.0	151.9	49.9	201.6

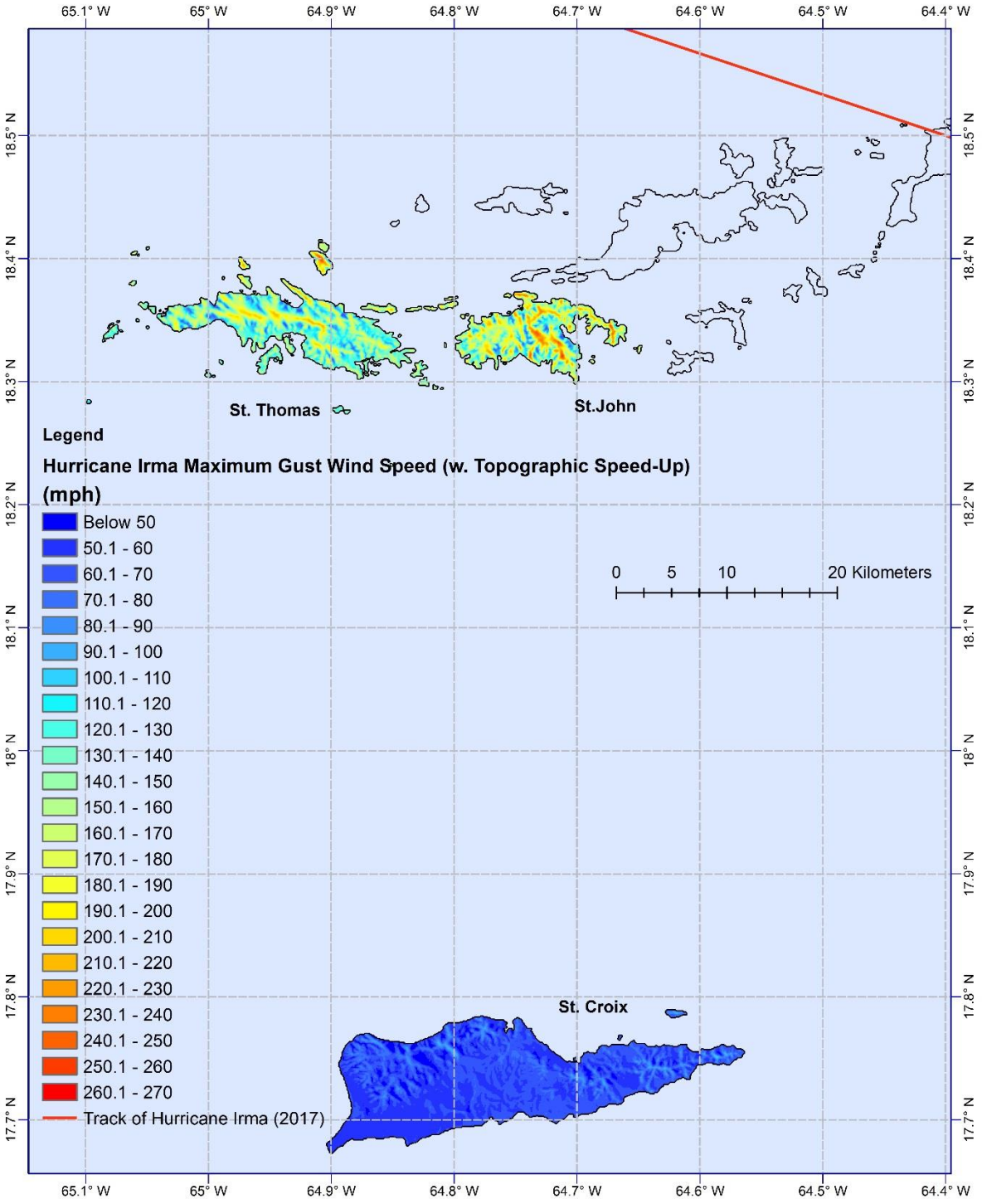

Figure 27. Map of USVI showing track of Hurricane Irma (2017) and estimated maximum peak gust wind speeds at a height of 10 m in open terrain. Wind speed estimates include the effect of topographic speed-ups.

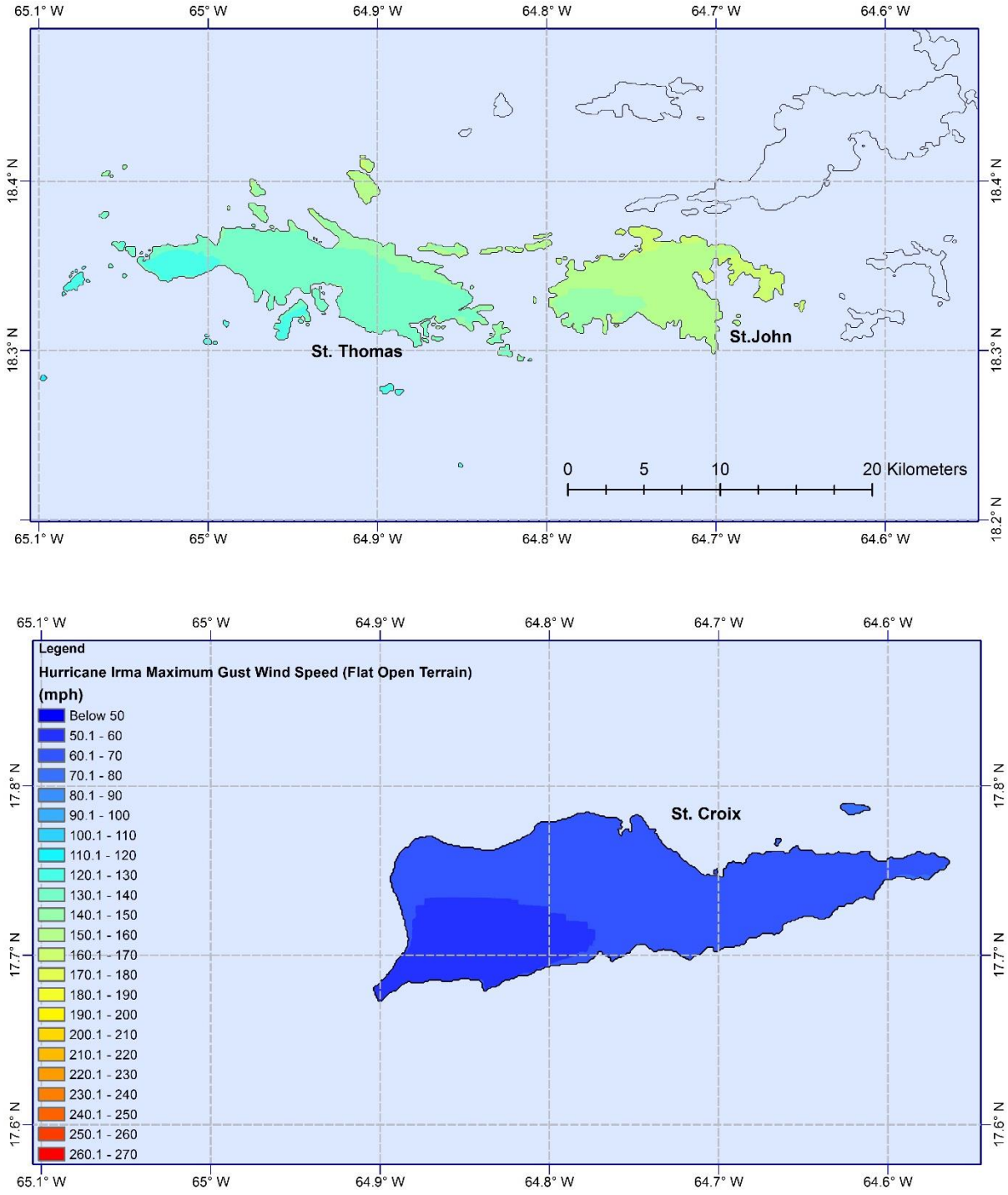

Figure 28. Close-up maps of USVI showing estimated maximum peak gust wind speeds at a height of 10 m in flat open terrain produced by Hurricane Irma (2017).

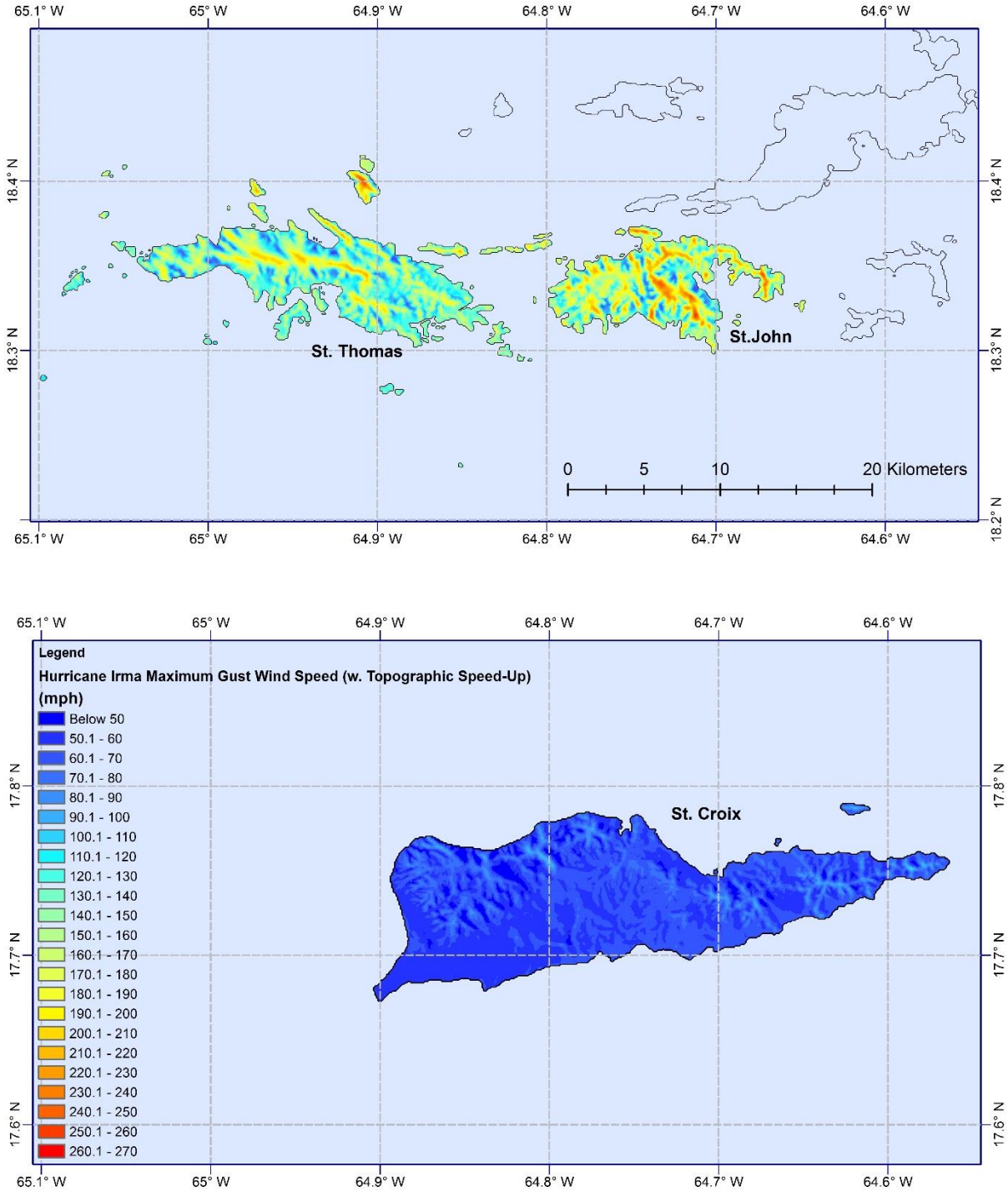

Figure 29. Close-up maps of USVI showing estimated maximum peak gust wind speeds at a height of 10 m in open terrain, including the effect of topographic speed-ups, produced by Hurricane Irma (2017).

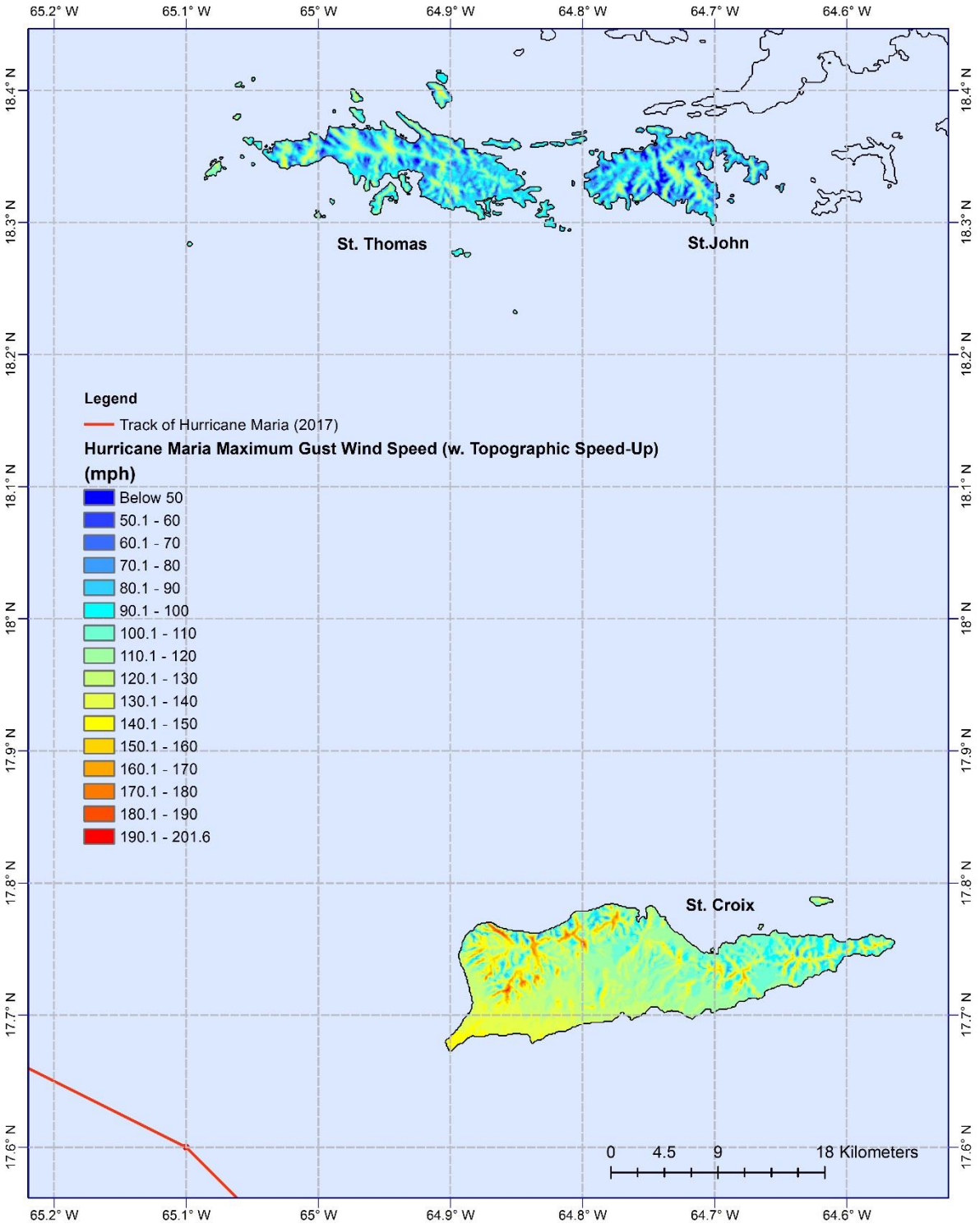

Figure 30. Map of USVI showing track of Hurricane Maria (2017) and estimated maximum peak gust wind speeds at a height of 10 m in open terrain. Wind speed estimates include the effect of topographic speed-ups.

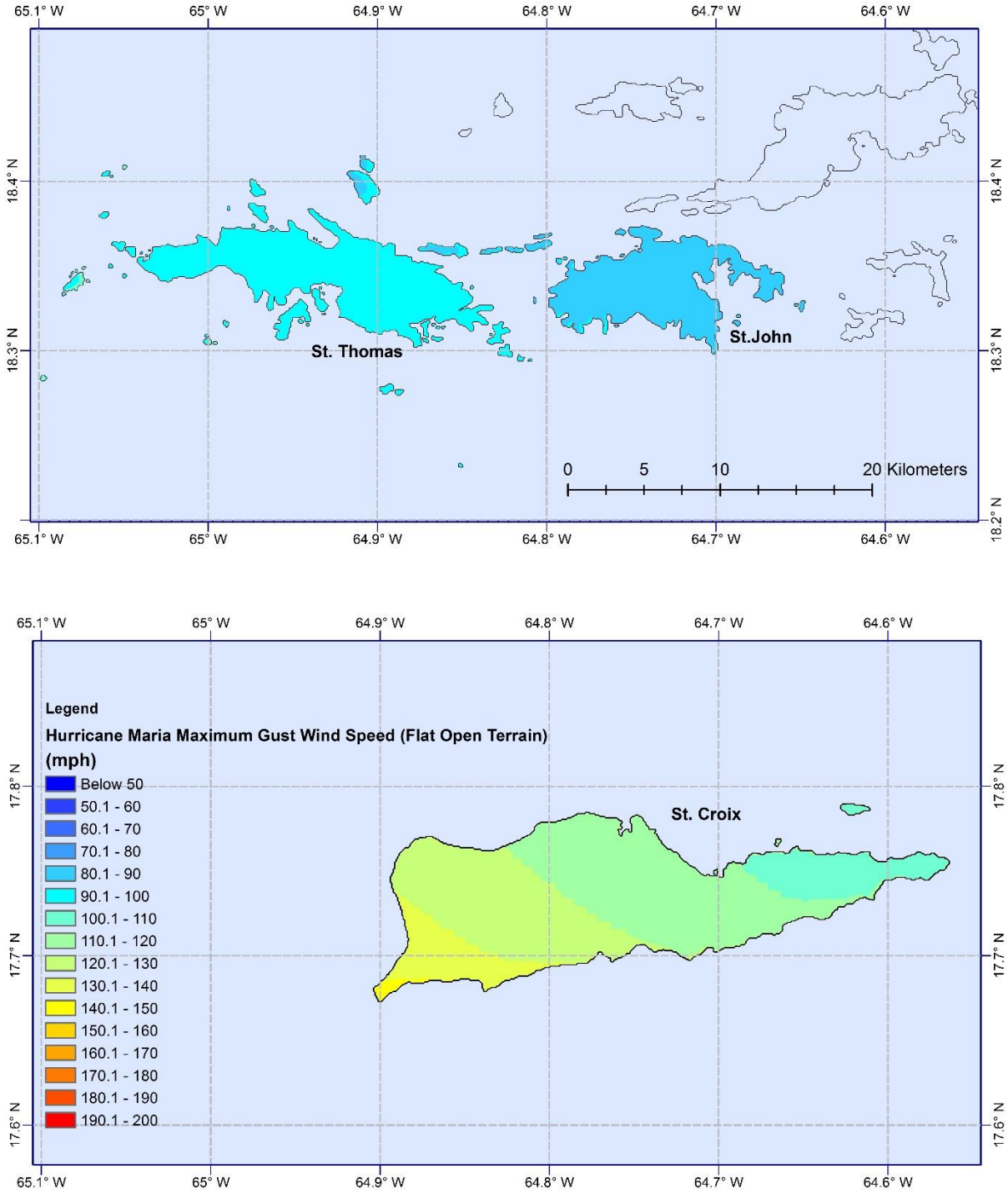

Figure 31. Close-up maps of USVI showing estimated maximum peak gust wind speeds at a height of 10 m in flat open terrain produced by Hurricane Maria (2017).

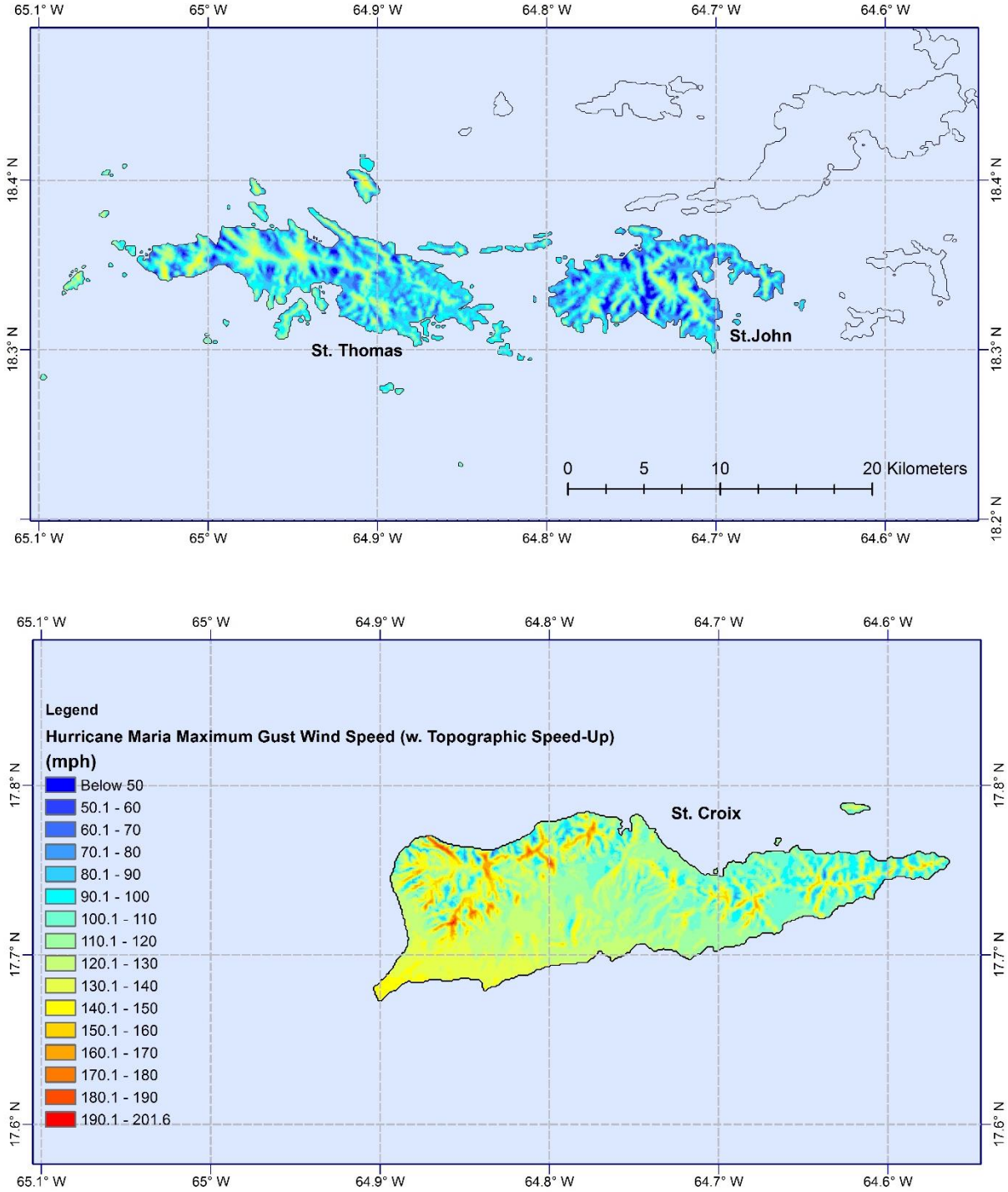

Figure 32. Close-up maps of USVI showing estimated maximum peak gust wind speeds at a height of 10 m in open terrain, including the effect of topographic speed-ups, produced by Hurricane Maria (2017).

References

Applied Research Associates, Inc. (2001) *Hazard Mitigation Study for the Hawaii Hurricane Relief Fund,* ARA Report 0476, Raleigh, NC. https://www.google.com/search?q=Hazard+Mitigation+Study+for+the+Hawaii+Hurricane+Relief+Fund&oq=Hazard+Mitigation+Study+for+the+Hawaii+Hurricane+Relief+Fund&aqs=chrome..69i57.485j0j4&sourceid=chrome&ie=UTF-8

Bechmann, A, N. N. Sorenson, J. Berg, J. Mann and P. E. Rethore (2011) "The Bolund experiment, part II: blind comparison of microscale flow models" *Boundary-Layer Meteorol*. **141** pp 245-271

Berg J, J. Mann, A. Bechmann, M, J. Courtney and H. E. Jorgensen H (2011) "The Bolund experiment, part I: flow over a steep, three-dimensional hill", *Boundary-Layer Meteorol*. **141** pp 219-243

Chock, G., J. Peterka, J. and L. Cochran (2000) "*Orographically amplified wind loss models for Hawaii and Pacific Insular States*", Prepared for NASA Goddard Space Flight Center, Headquarters Procurement Office, Code 201.H, Greenbelt, MD 20771, NASA Contract NASA-99045

Chock, G, J. and L. Cochran (2006) "Erratum to Modeling of Topographic Wind Effects in Hawaii", *J. Wind Eng. Ind. Aerodyn.* **94**, 173-187

Chock, G, J. Peterka, J. and G. Yu (2005) "Topographic wind speed-up and directionality factors for use in the city and county of Honolulu building code", *Proc.10th Americas Conf. on Wind Eng.*, Louisiana State University, Baton Rouge, LA. http://martinchock.com/_library/documents/papers/presentations/topographicwindspeed-upanddirectionalityfactorsforthe.pdf

Vickery, P. J. and D. Wadhera (2008) "*Development of design wind speed maps for application with the wind load provisions of ASCE 7*" Pan American Health Organization, 525 23rd Street NW, Washington, DC 20073-2875 https://www.paho.org/disasters/index.php?option=com_docman&view=download&category_slug=safe-hospitals&alias=550-methodology-used-for-wind-hazard-maps&Itemid=1179&lang=en

Appendix A.

Maps Showing Topographic Speed-ups for all Sixteen Wind Directions

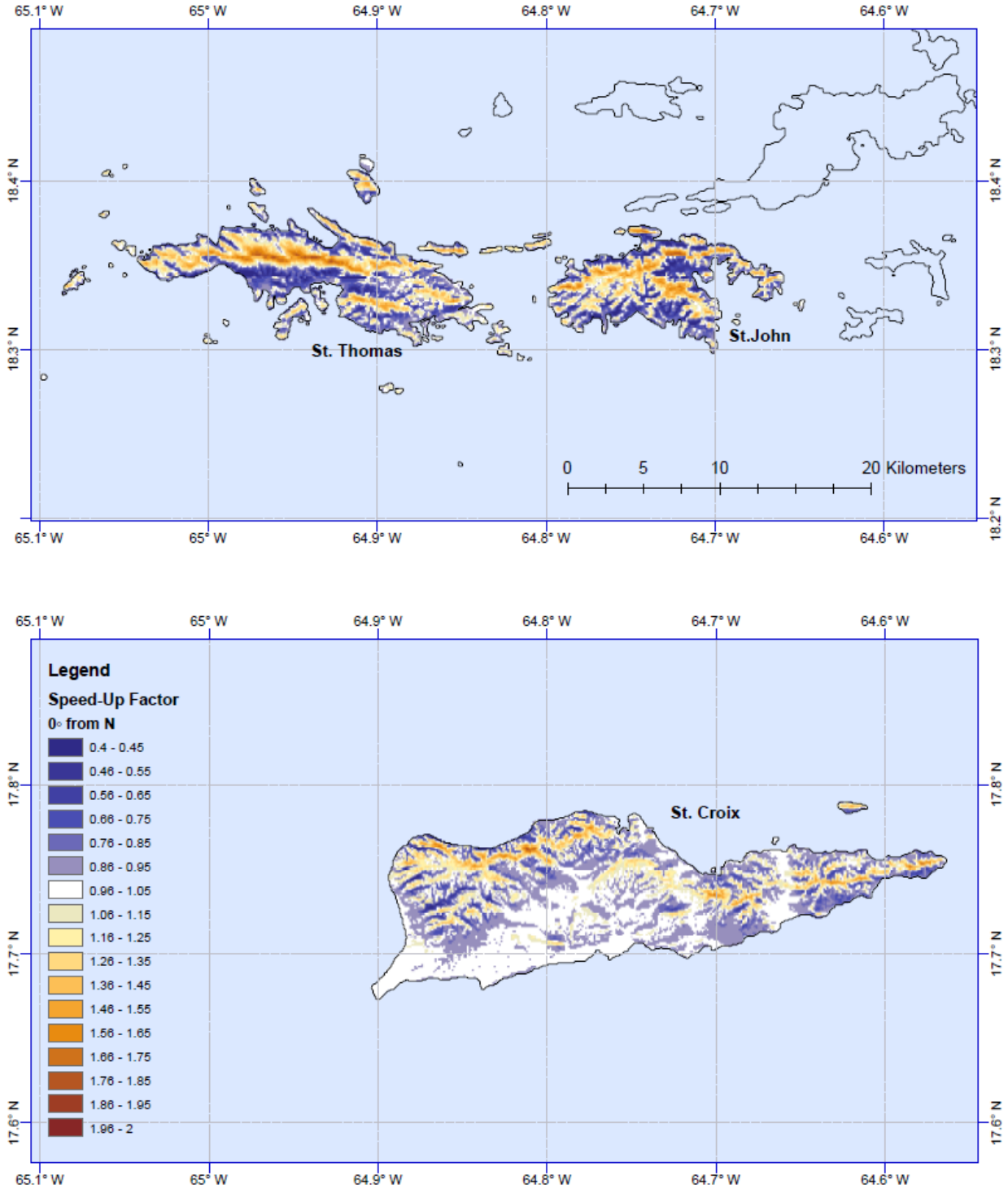

Figure A-1. Wind speed-ups for winds approaching from the north (0°)

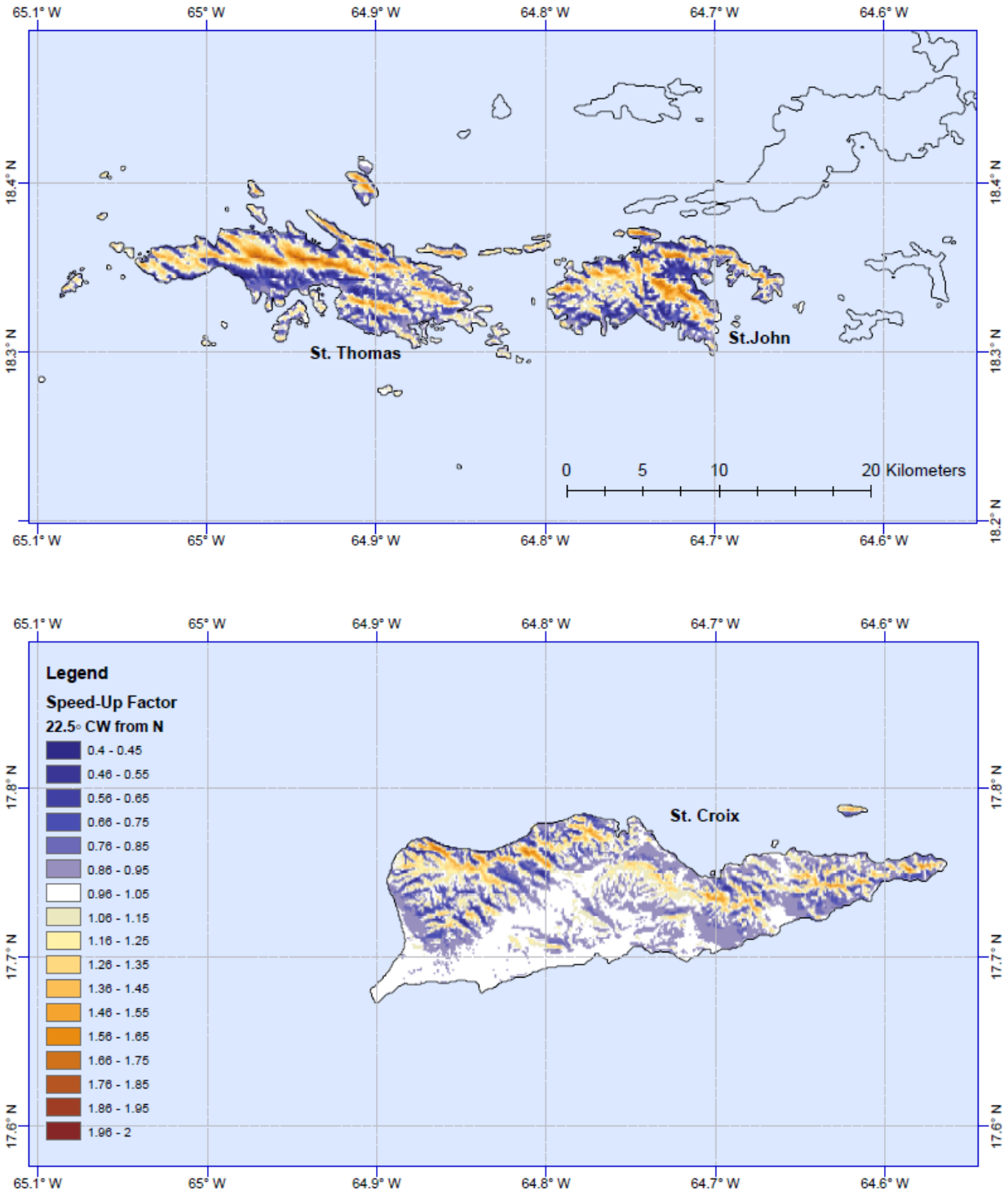

Figure A-2. Wind speed-ups for winds approaching from the north-north-east (22.5°)

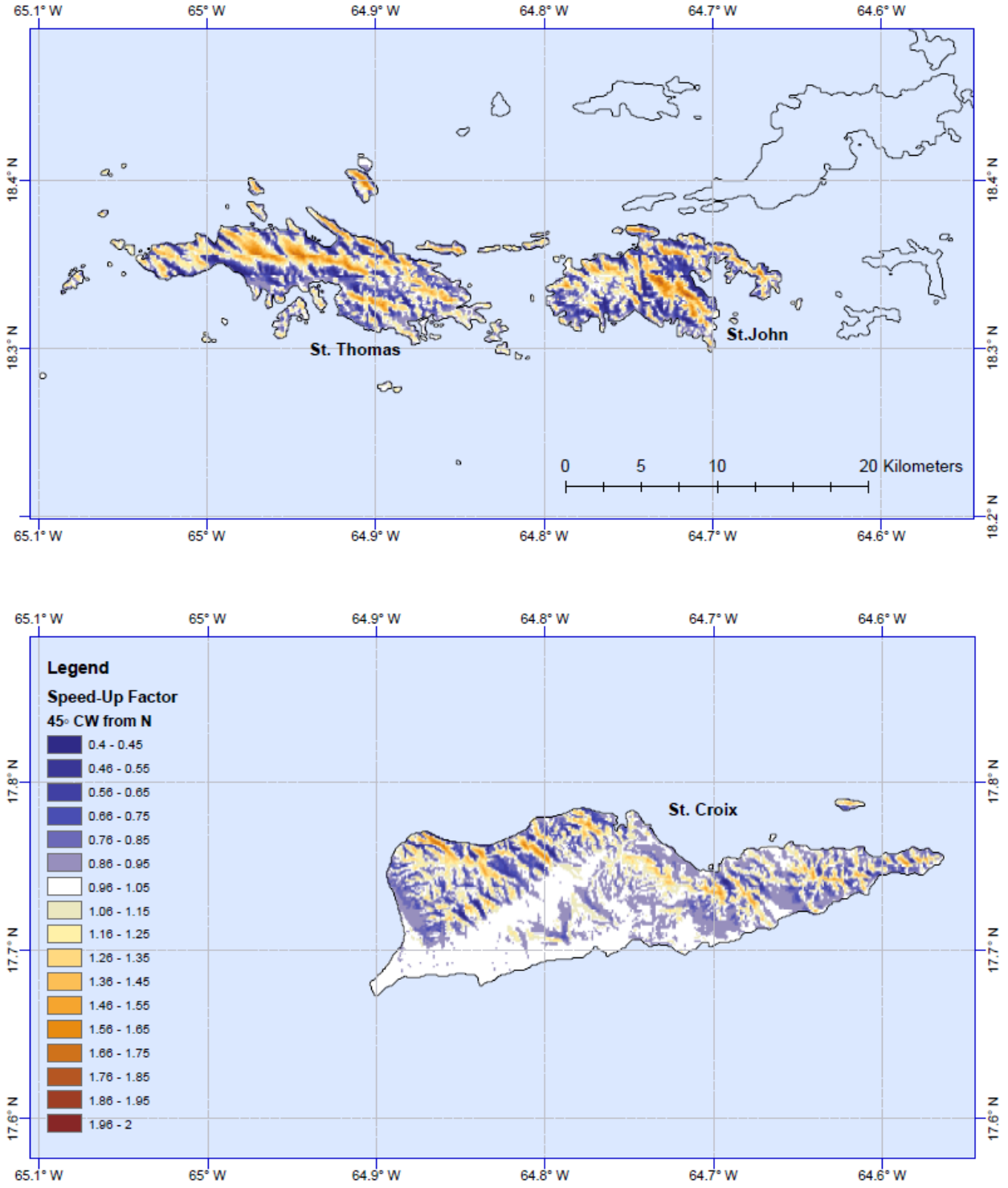

Figure A-3. Wind speed-ups for winds approaching from the north-east (45°)

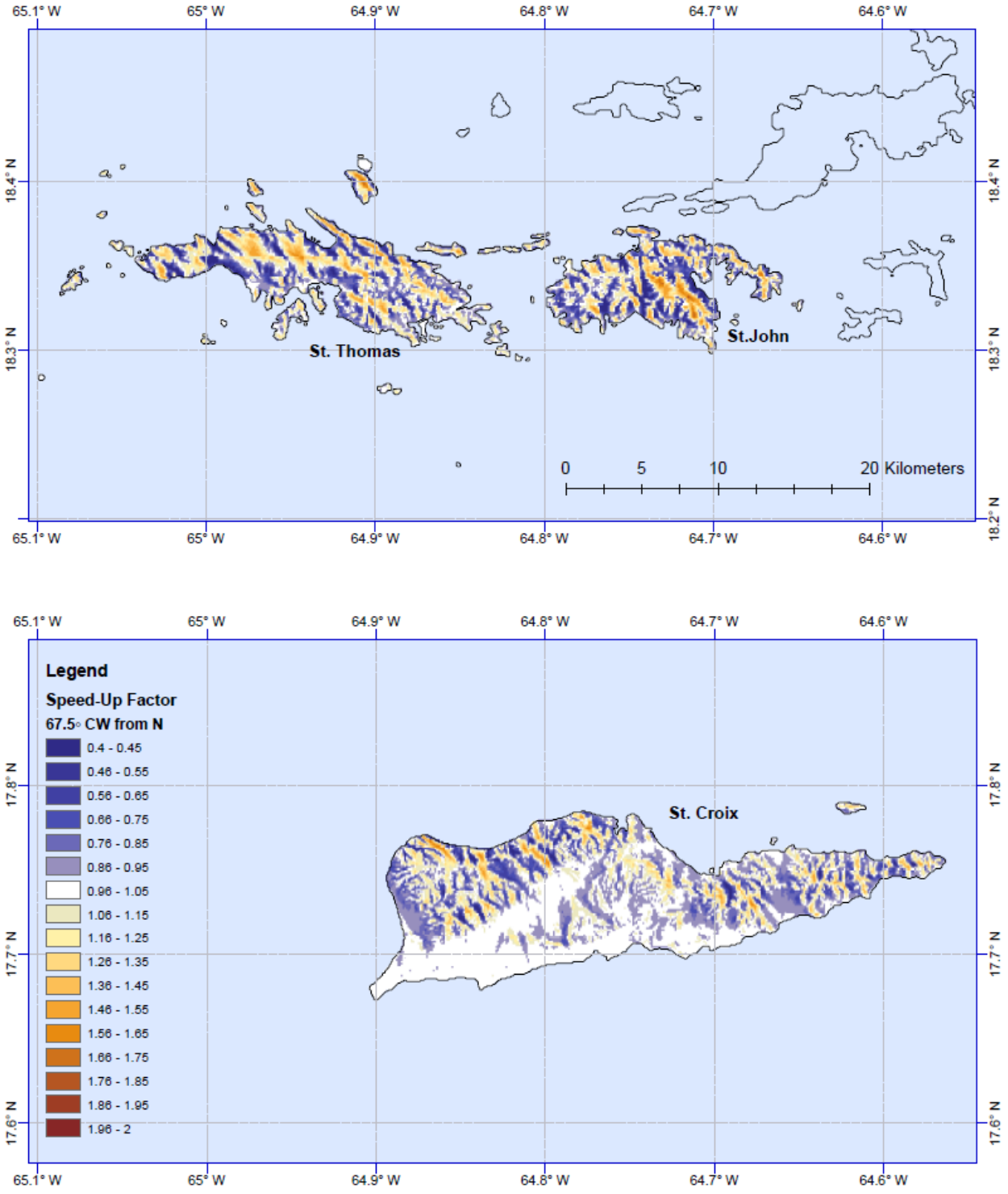

Figure A-4. Wind speed-ups for winds approaching from the east-south-east (67.5°)

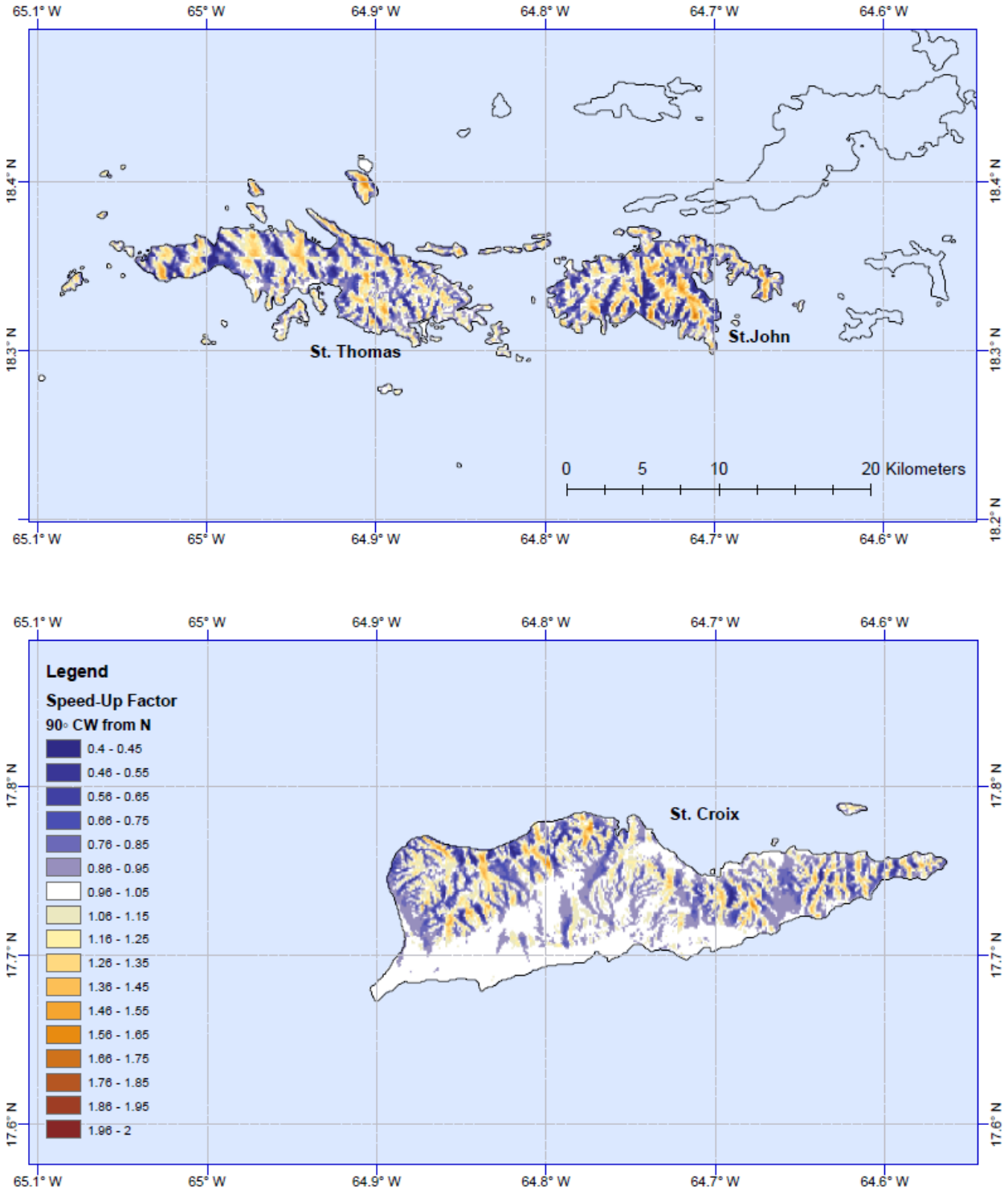

Figure A-5. Wind speed-ups for winds approaching from the east (90°)

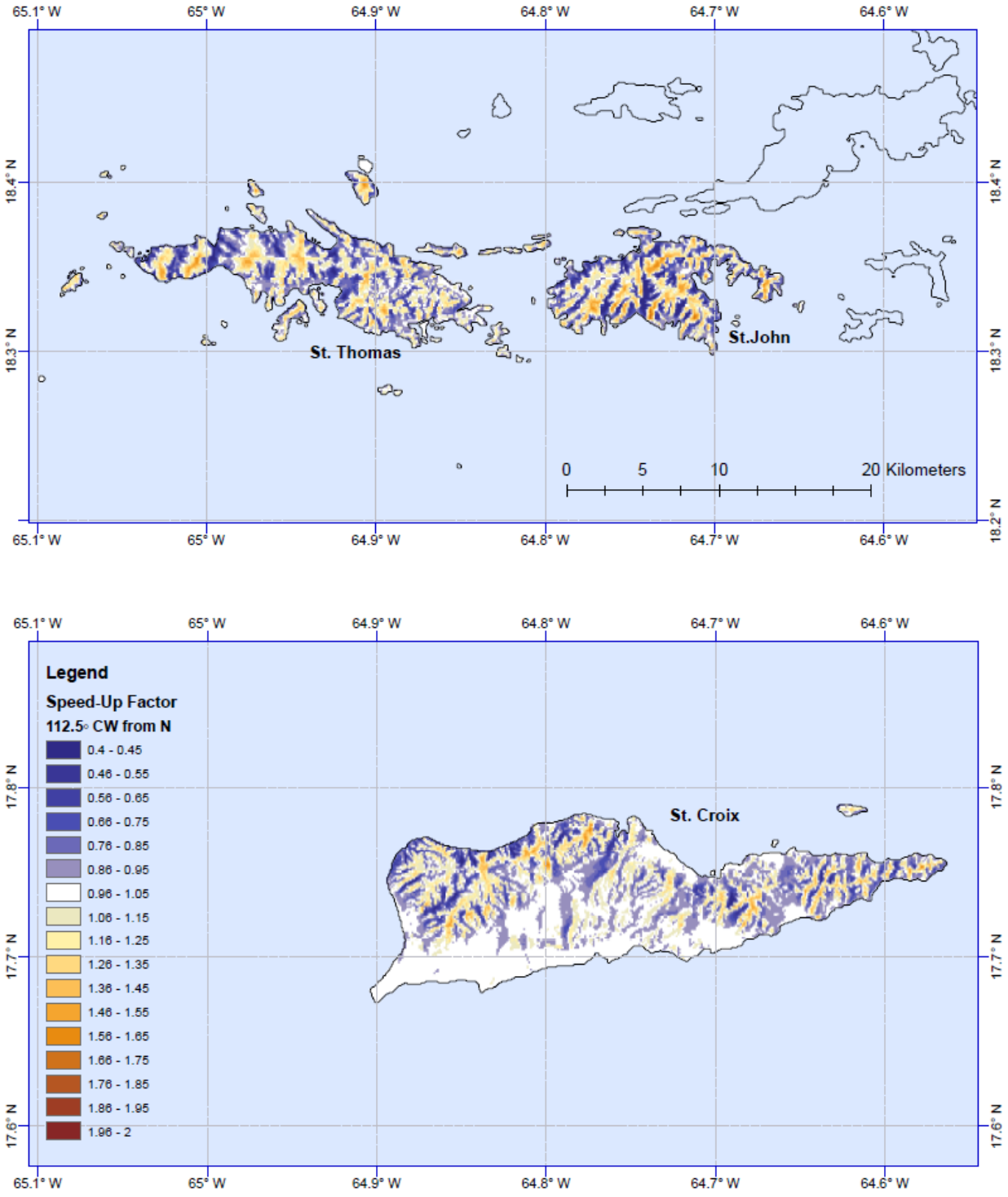

Figure A-6. Wind speed-ups for winds approaching from the east-southeast (112.5°)

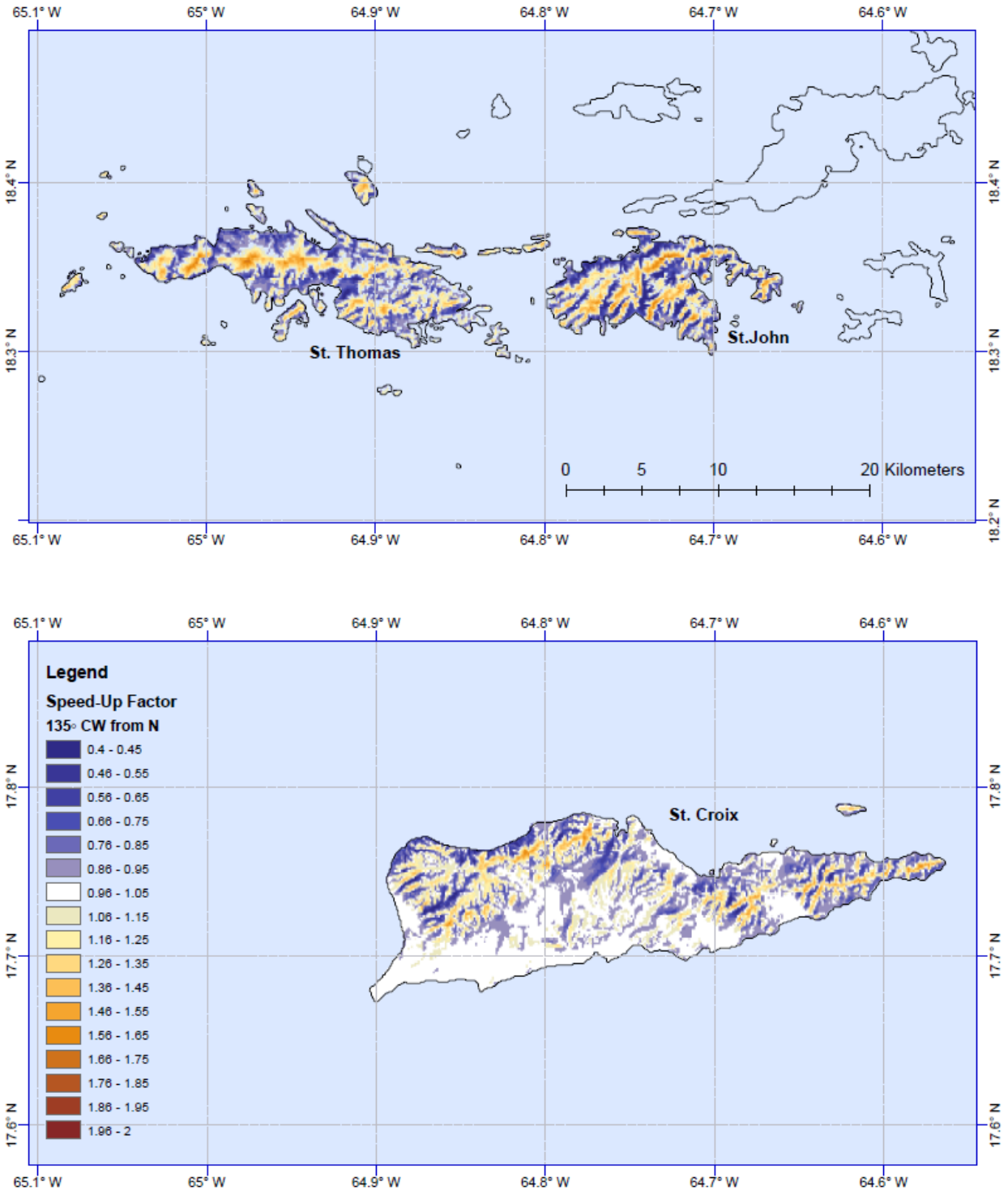

Figure A-7. Wind speed-ups for winds approaching from the southeast (135°)

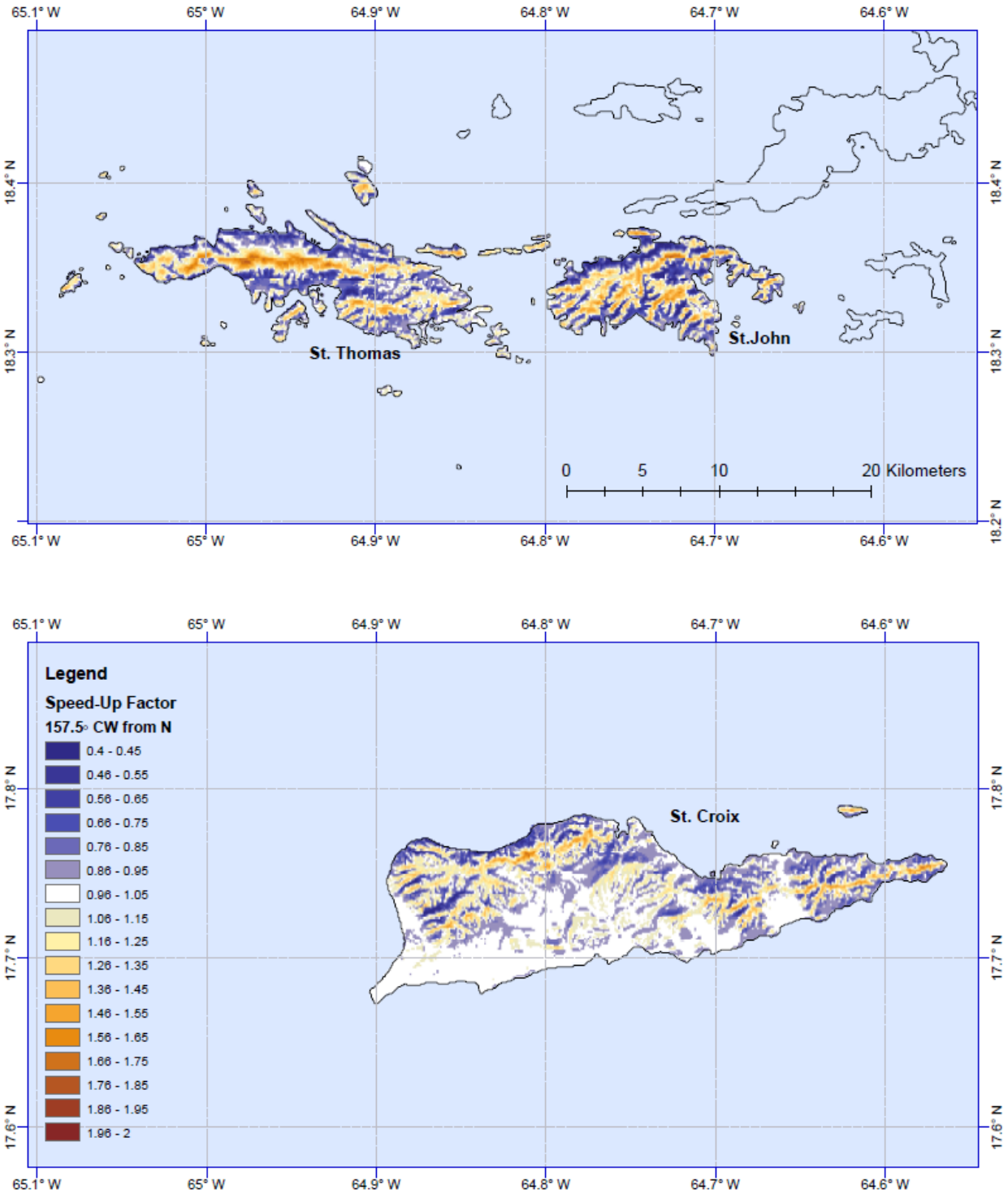

Figure A-8. Wind speed-ups for winds approaching from the south-southeast (157.5°)

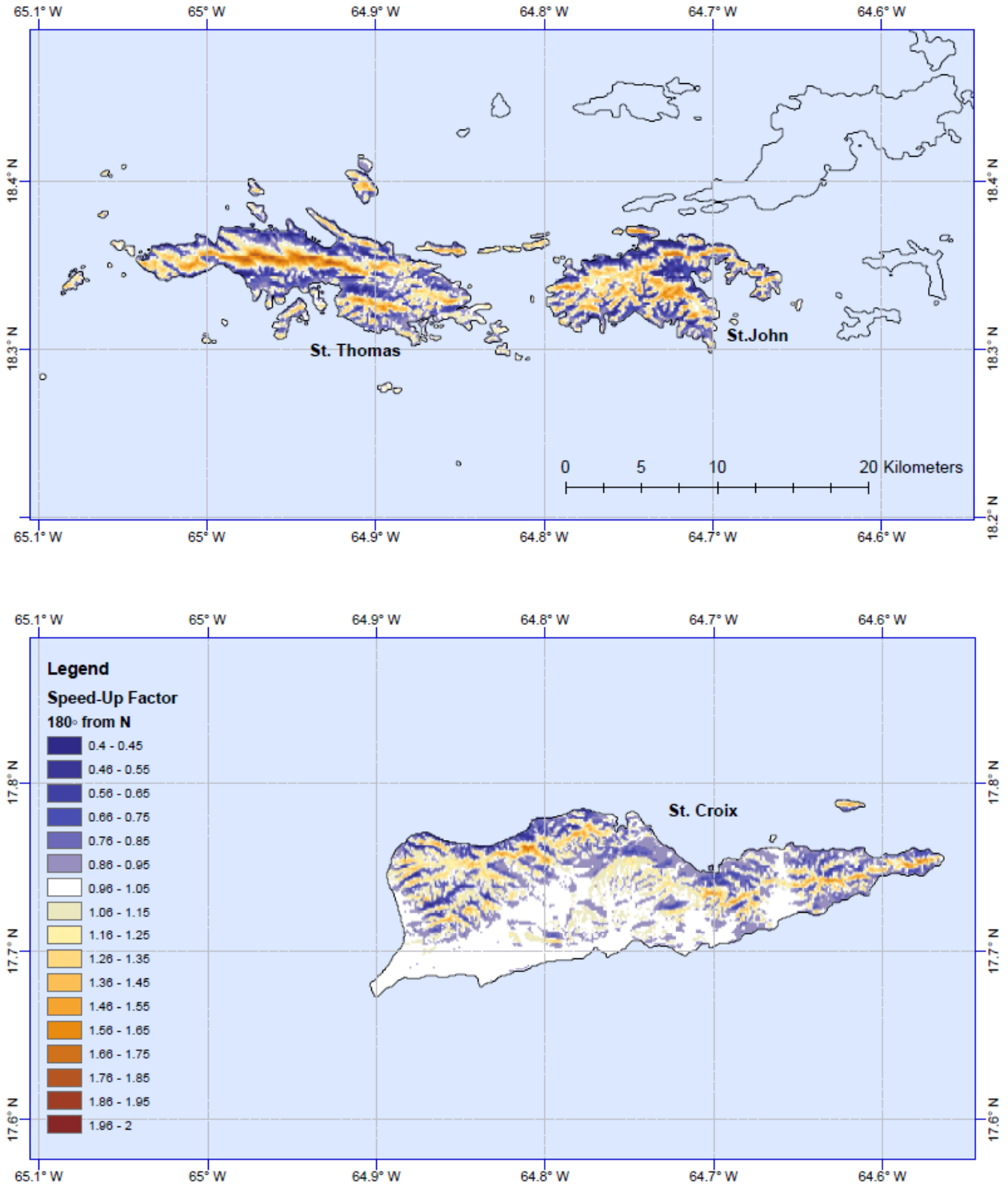

Figure A-9. Wind speed-ups for winds approaching from the south (180°)

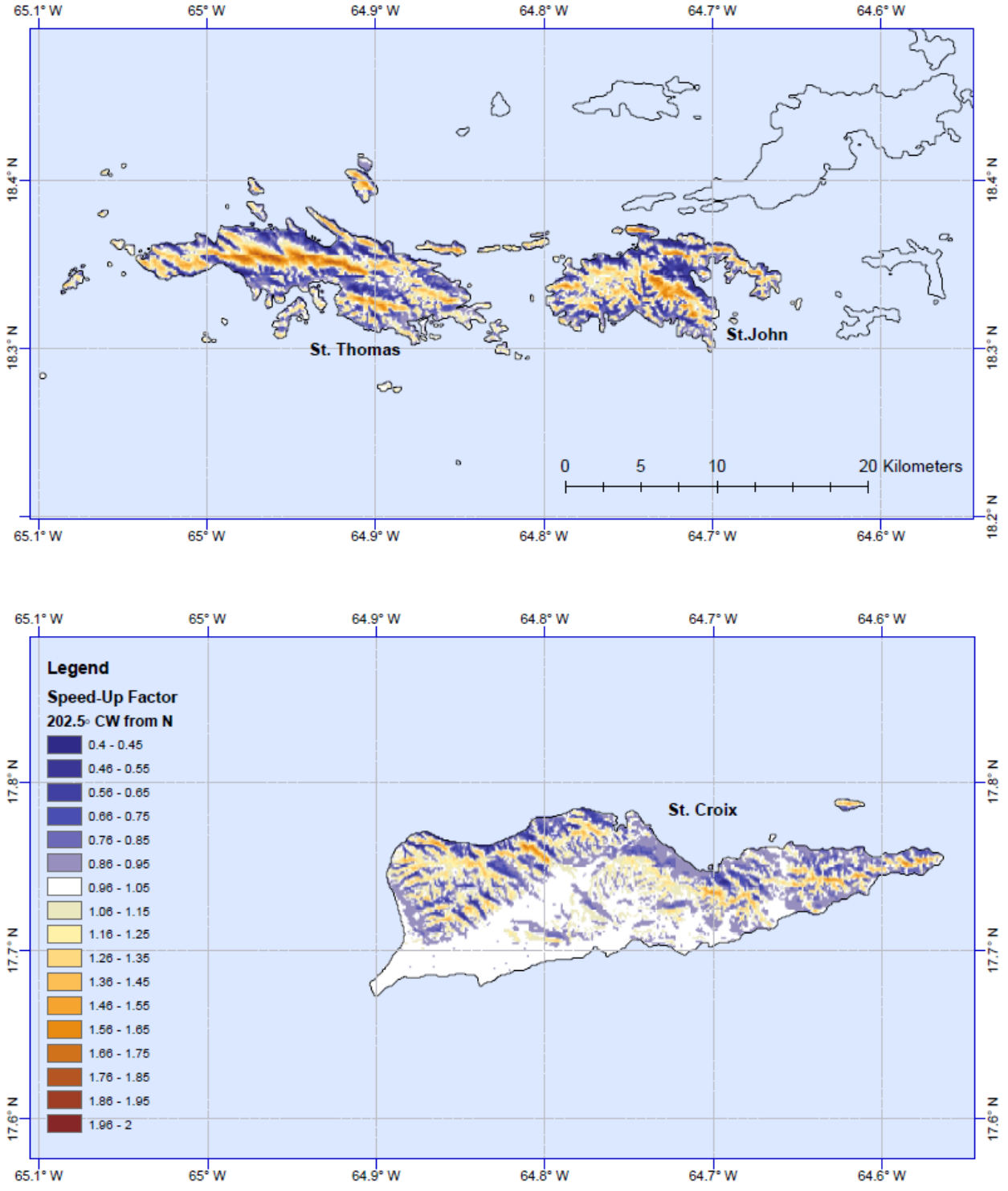

Figure A-10. Wind speed-ups for winds approaching from the south-southwest (202.5°)

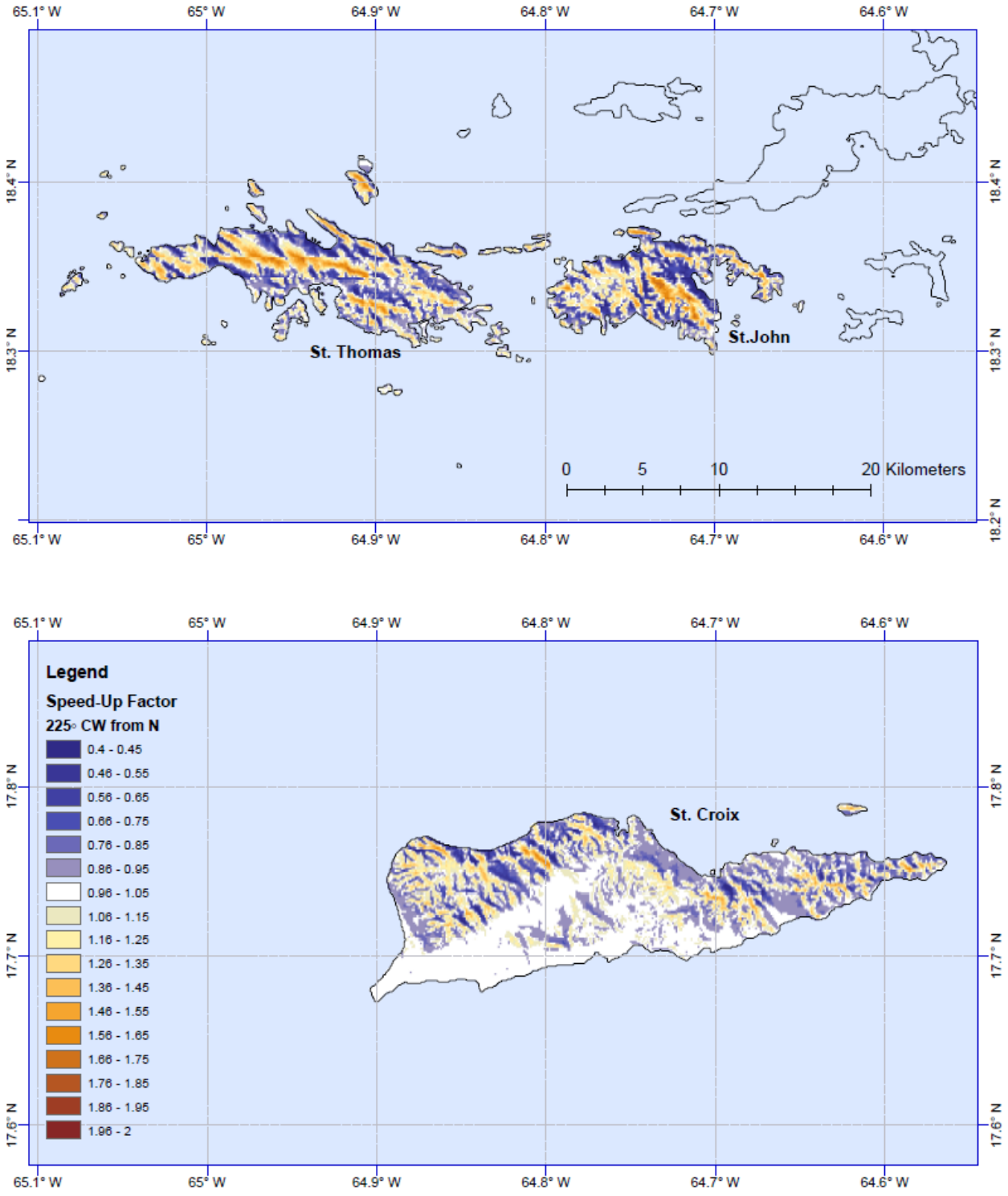

Figure A-11. Wind speed-ups for winds approaching from the southwest (225°)

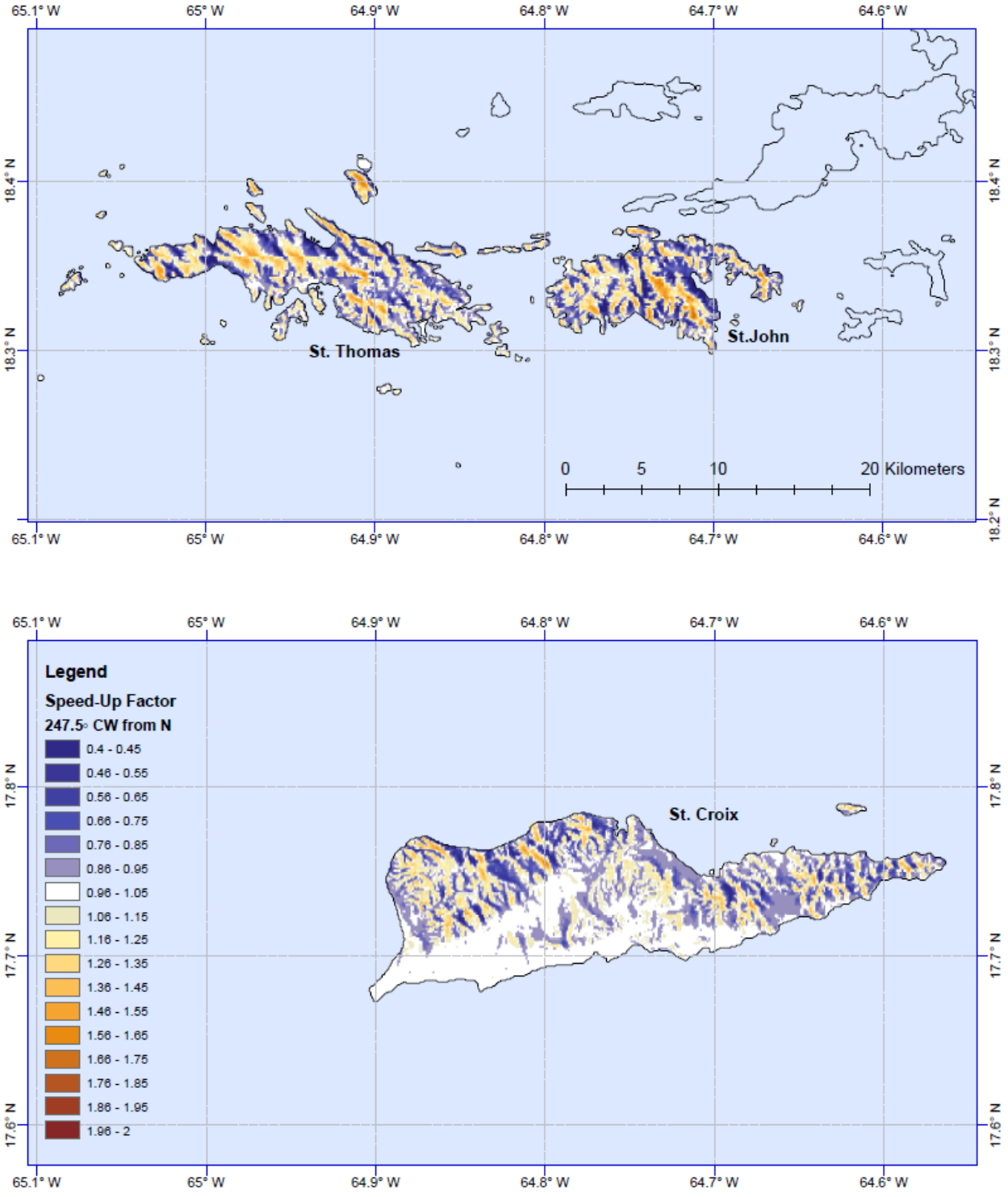

Figure A12. Wind speed-ups for winds approaching from the west-southwest (247.5°)

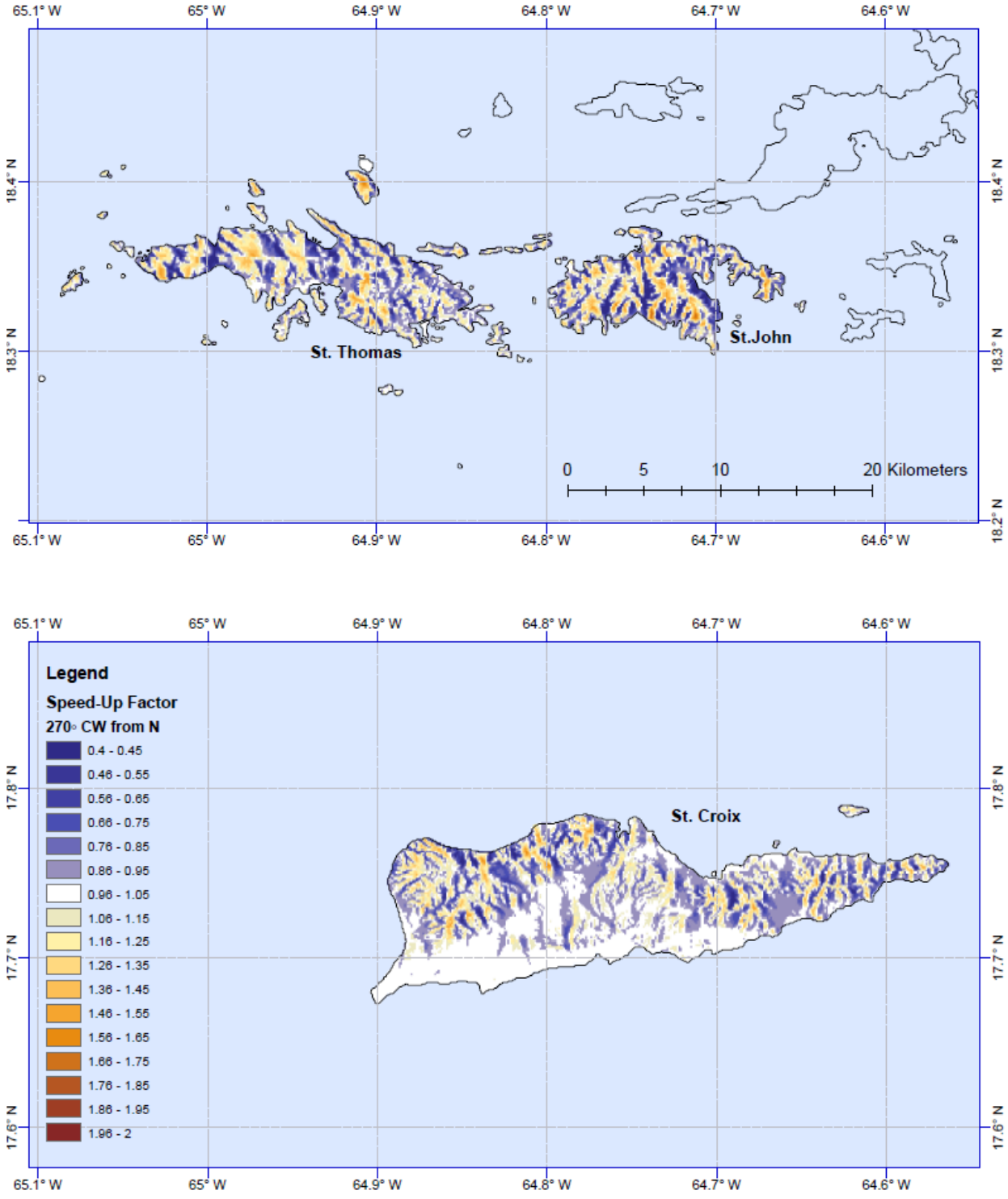

Figure A13. Wind speed-ups for winds approaching from the west (270°)

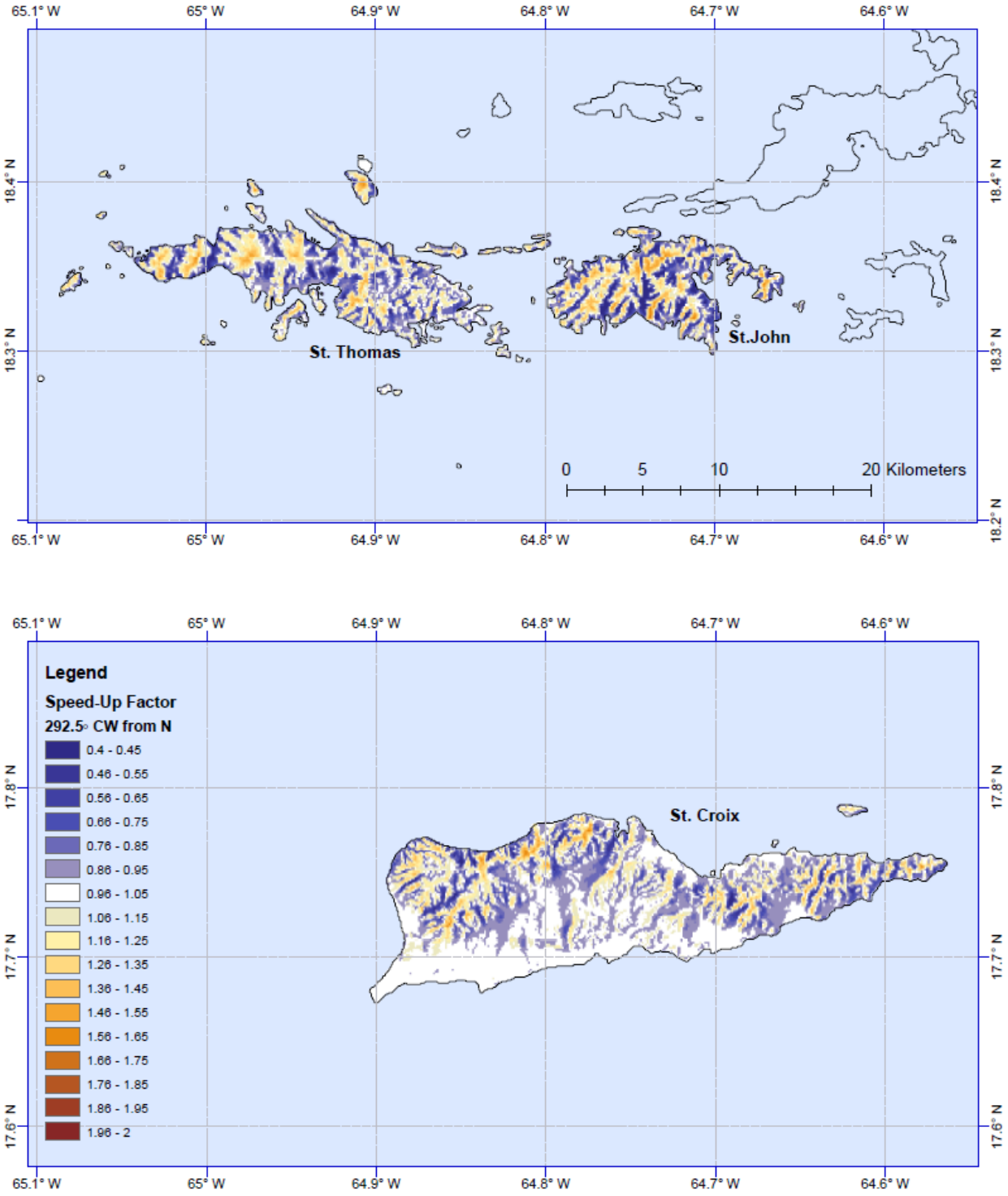

Figure A14. Wind speed-ups for winds approaching from the west-northwest (292.5°)

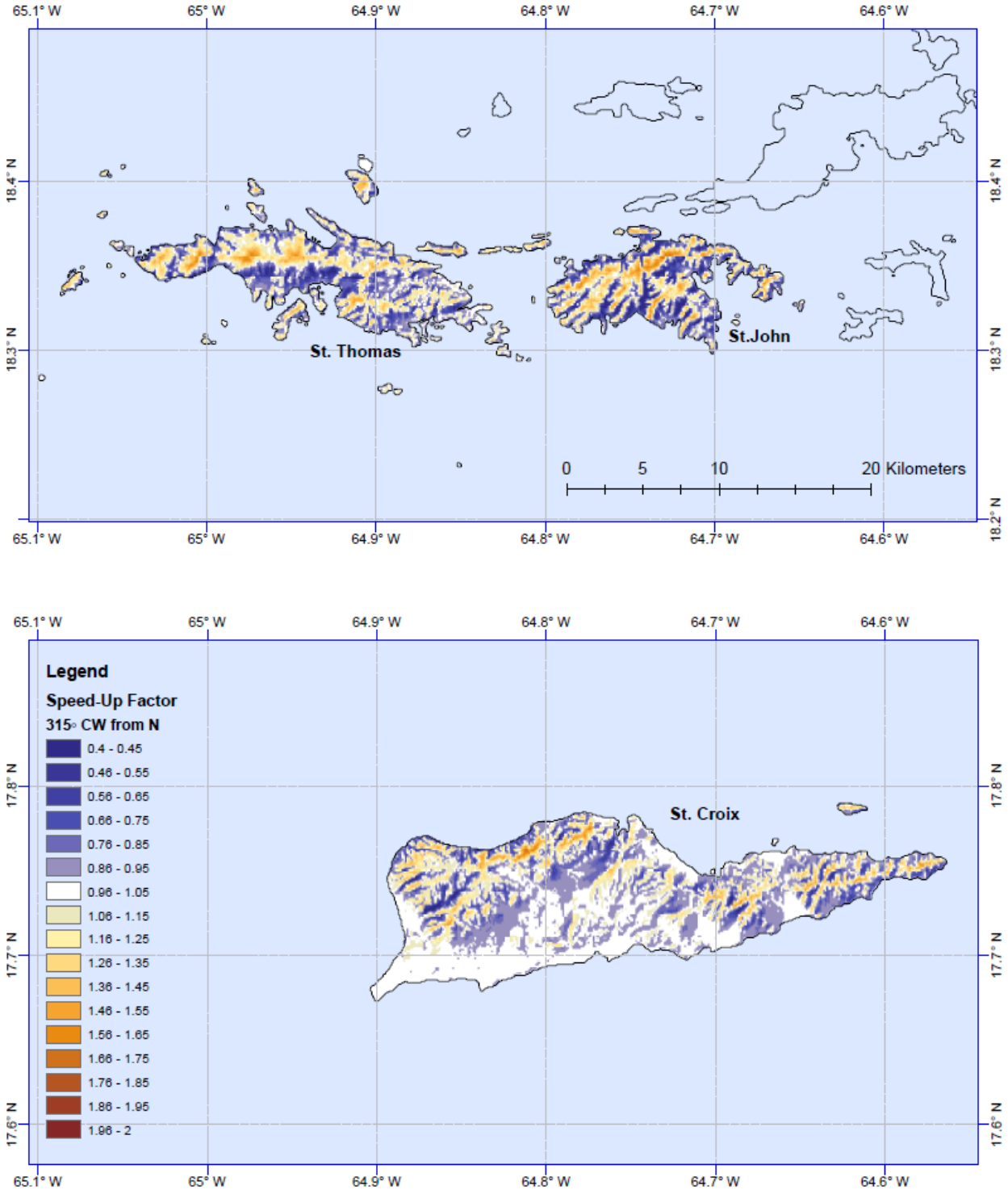

Figure A15. Wind speed-ups for winds approaching from the northwest (315°)

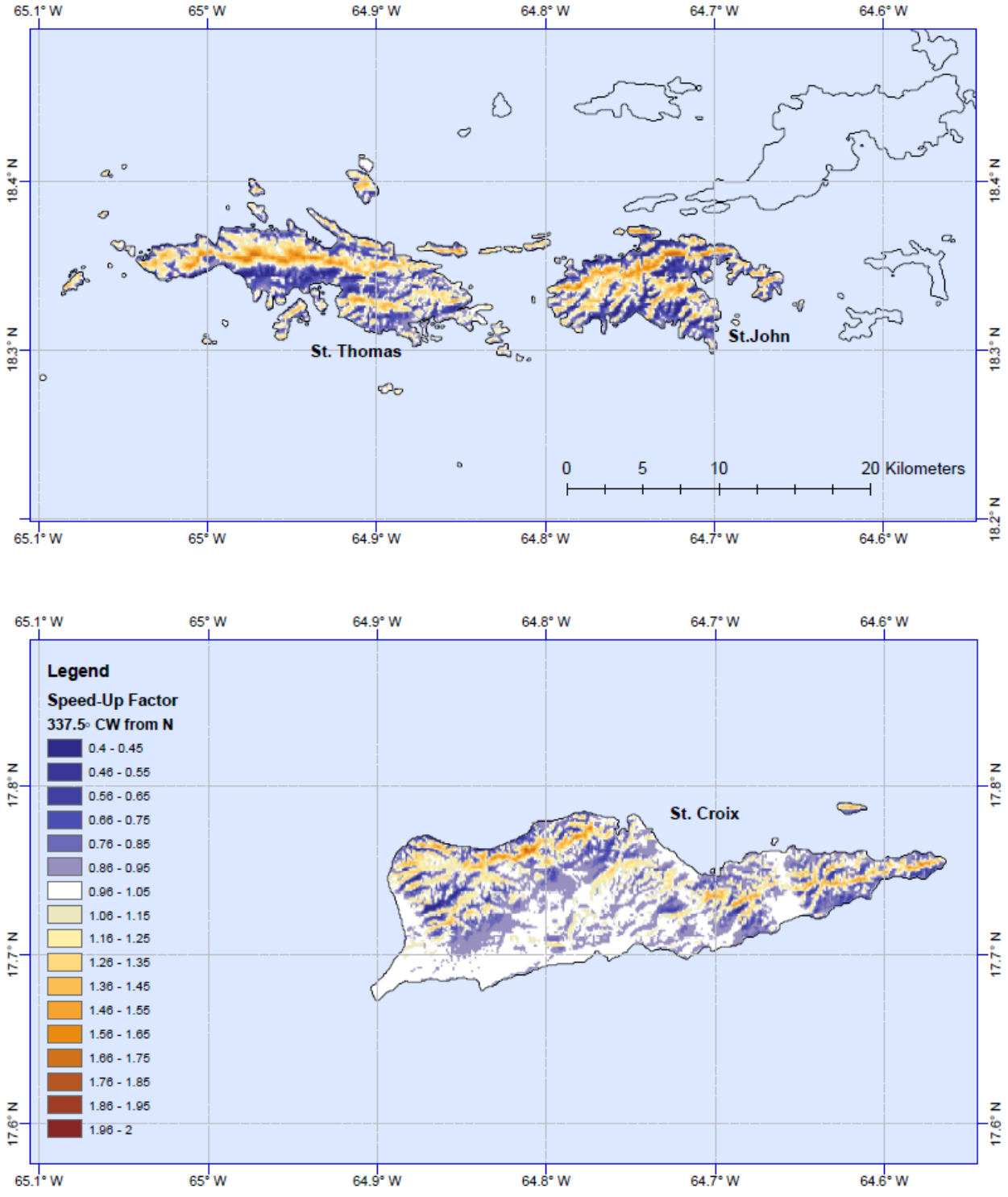

Figure A16. Wind speed-ups for winds approaching from the north-northwest (337.5°)

Appendix B.

Maps Showing Predicted 3-Second Gust Wind Speeds for Various Return Periods for the USVI. Wind Speeds are given at a Height of 10 m in Flat Open Terrain.

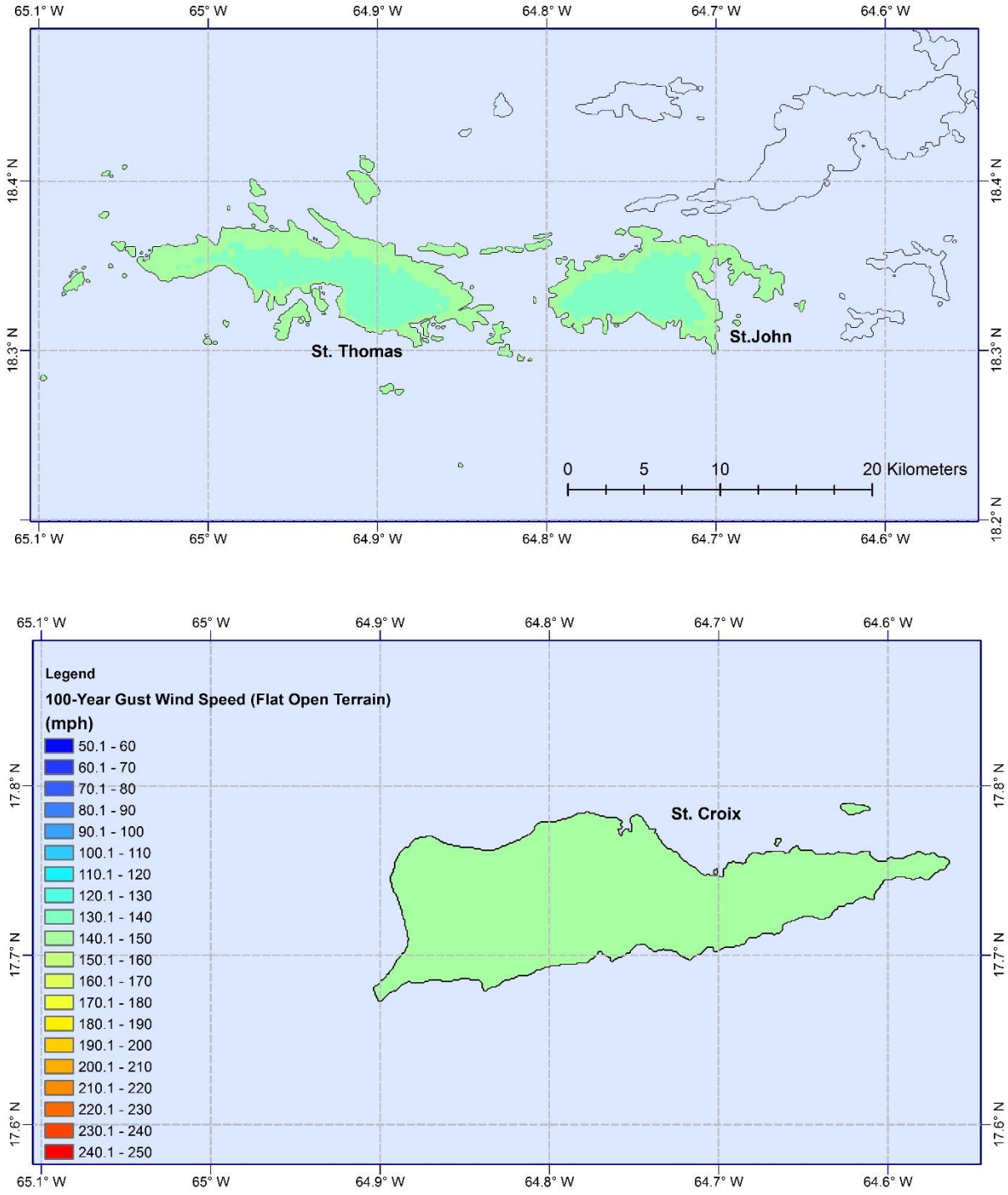

Figure B1. 100-year return period 3-second gust wind speeds for the USVI in flat open terrain. Wind speeds are valid for a height of 10 m.

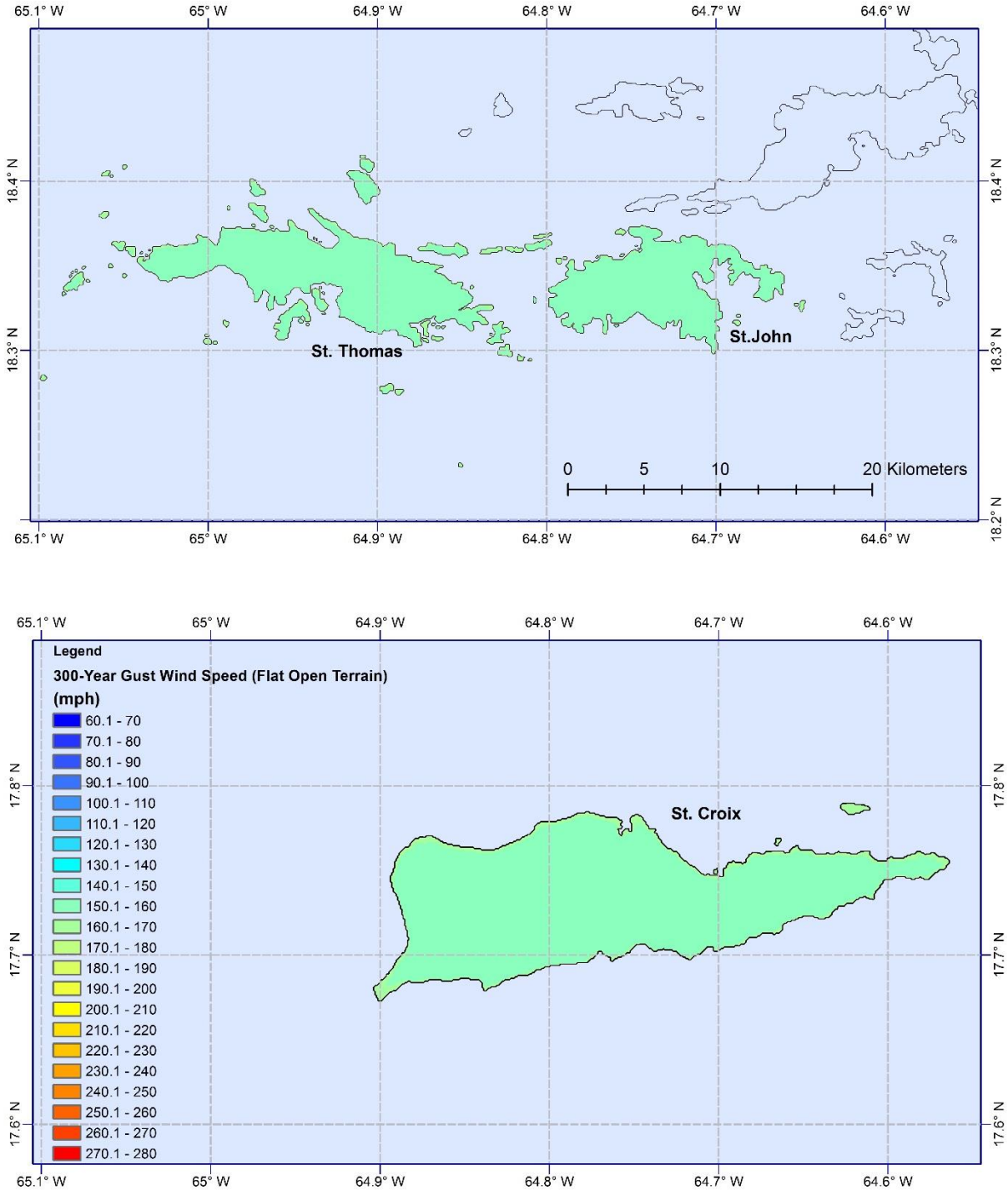

Figure B2. 300-year return period 3-second gust wind speeds for the USVI in flat open terrain. Wind speeds are valid for a height of 10 m.

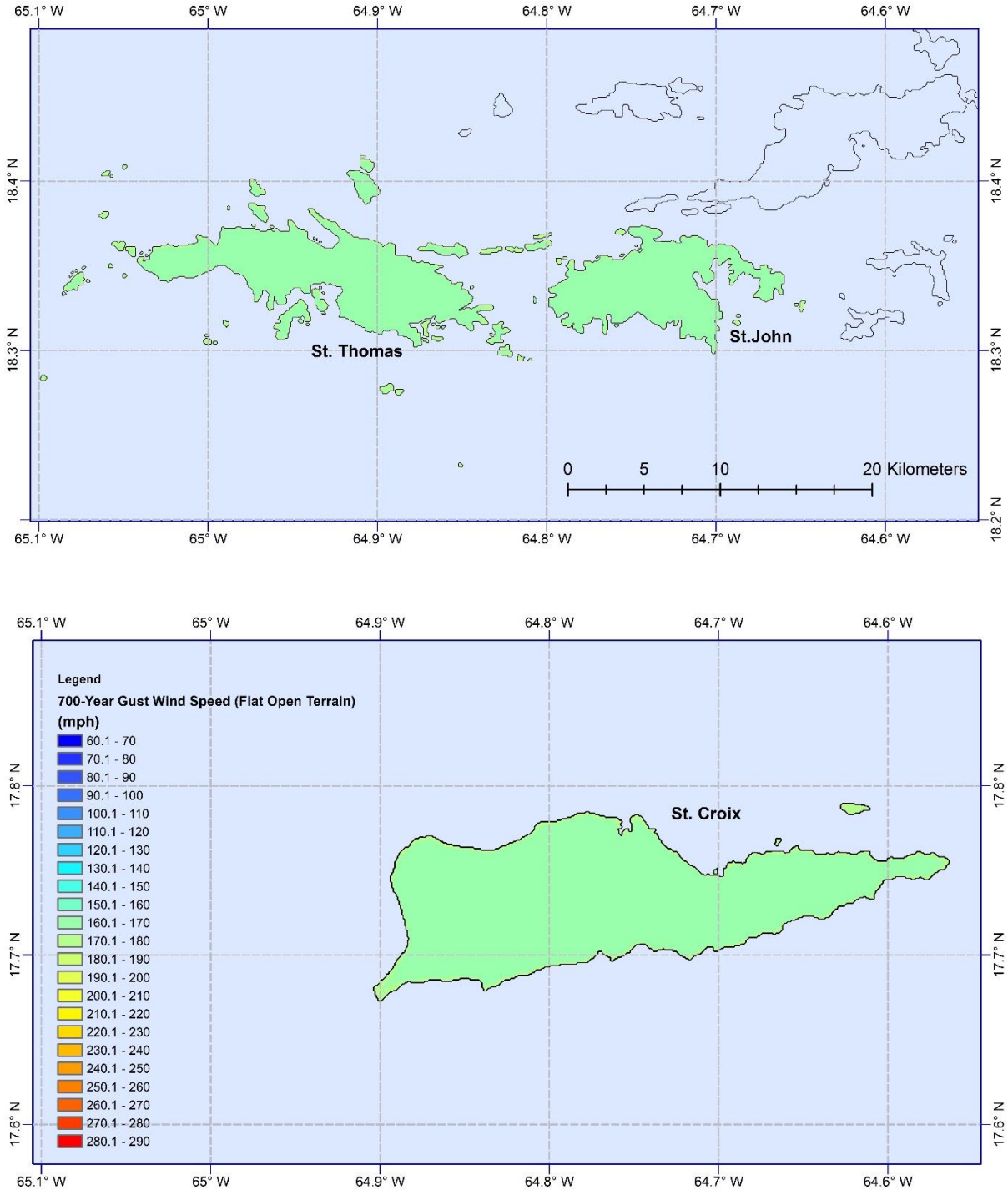

Figure B3. 700-year return period 3-second gust wind speeds for the USVI in flat open terrain. Wind speeds are valid for a height of 10 m.

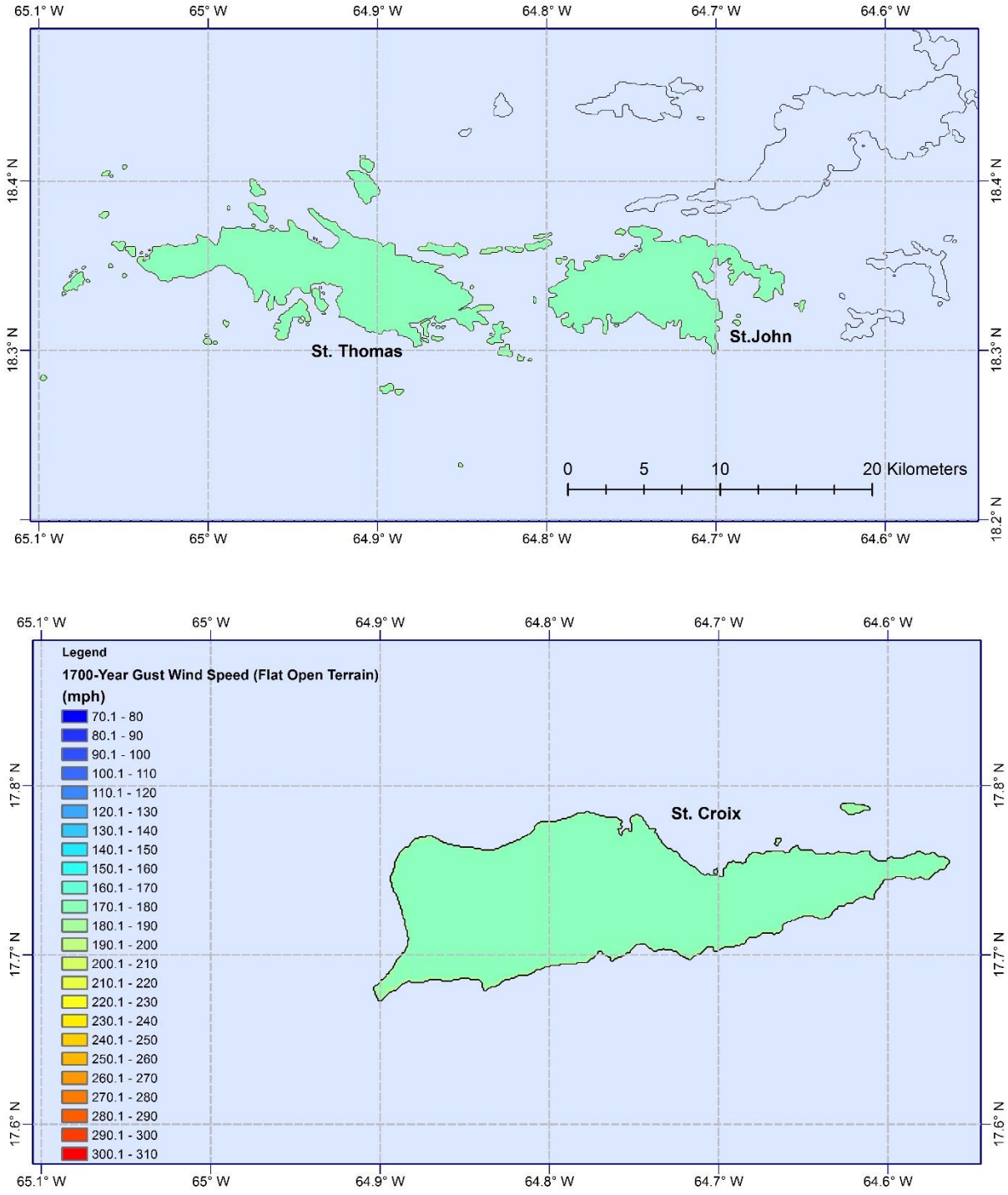

Figure B4. 1,700-year return period 3-second gust wind speeds for the USVI in flat open terrain. Wind speeds are valid for a height of 10 m.

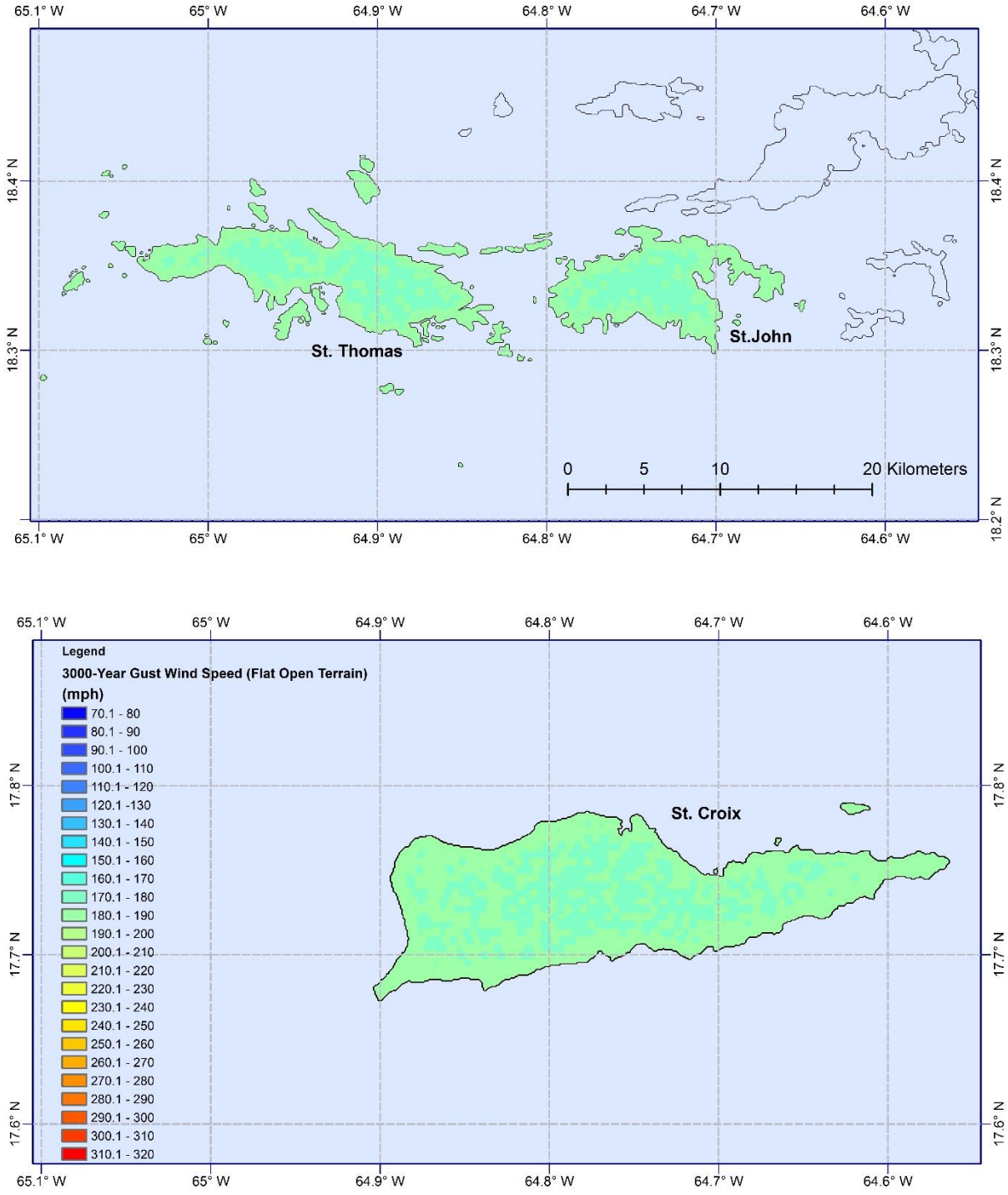

Figure B5. 3,000-year return period 3-second gust wind speeds for the USVI in flat open terrain. Wind speeds are valid for a height of 10 m.